

1 **A synoptic survey of young mesoscale eddies in the**
2 **Eastern Gulf of Alaska**

3 Carol Ladd¹, William R. Crawford², Colleen E. Harpold³, W. Keith Johnson², Nancy B.
4 Kachel⁴, Phyllis J. Stabeno¹, Frank Whitney²

5 *¹Pacific Marine Environmental Laboratory, NOAA, 7600 Sand Point Way, Seattle, WA,*
6 *USA. 98115-6349*

7 *²Institute of Ocean Sciences, Fisheries and Oceans Canada, P.O. Box 6000, Sidney, BC,*
8 *Canada V8L 4B2*

9 *³Alaska Fisheries Science Center, NOAA, 7600 Sand Point Way, Seattle, WA, USA*
10 *98115-6349*

11 *⁴Joint Institute for the Study of the Atmosphere and Ocean, University of Washington,*
12 *Box 357941, Seattle, WA, USA 98195*

13 *Corresponding author:*

14 *C. Ladd*

15 *e-mail: carol.ladd@noaa.gov*

16 *phone: (206) 526-6024*

17 *fax: (206) 526-6485*

18 **Abstract**

19 Eddies in the Gulf of Alaska are important sources of coastal water and associated
20 nutrients, iron, and biota to the high nutrient, low chlorophyll central Gulf of Alaska.
21 Three primary eddy formation regions along the eastern boundary of the gulf have been
22 identified, (from south to north, Haida, Sitka, and Yakutat). In the spring of 2005, three
23 eddies (one of each type) were sampled soon after their formation. The subsurface eddy
24 core water in all three eddies was defined by high iron concentrations and low dissolved
25 oxygen compared with surrounding basin water. The Sitka and Yakutat core waters also
26 exhibited a subsurface temperature maximum (mesothermal water) coincident in depth
27 with the iron maximum, suggesting that eddies may play a role in the formation of
28 temperature inversions observed throughout the Gulf of Alaska. The data suggest
29 different formation regions, with the Yakutat eddy forming in shallow shelf water with
30 riverine input while the Sitka and Haida eddies appear to form in deeper water.

31 Key words: Oceanic eddies, Gulf of Alaska, nutrients, iron

32 **1. Introduction**

33 The circulation in the Gulf of Alaska (GOA), located in the northeast corner of the
34 subarctic North Pacific, is dominated by the cyclonic Alaska Gyre. The gyre is bounded
35 on the south by the eastward North Pacific Current which bifurcates near the coast of
36 North America to feed the southward flowing California Current and the northward
37 flowing Alaska Current. The broad, variable Alaska Current forms the eastern boundary

38 current of the Alaska Gyre. The western boundary current, the Alaskan Stream, flows
39 southwestward along the continental slope (Fig. 1).

40 The eastern boundary of the GOA spawns numerous, anticyclonic eddies that can persist
41 for years. These eddies influence physical and chemical water properties and biota in the
42 GOA. Three groups of eddies (Haida, Sitka, and Yakutat eddies) are primarily
43 distinguished by their formation regions (Gower, 1989; Gower and Tabata, 1993;
44 Okkonen *et al.*, 2001). These three eddy groups share many common features, including
45 anticyclonic rotation, ~200 km diameter, formation along the eastern and northern
46 boundary of the GOA, and westward translation.

47 Haida eddies usually form at Cape St. James, the southern tip of the Queen Charlotte
48 Islands, British Columbia (Crawford *et al.*, 2002; Di Lorenzo *et al.*, 2005). Formation of
49 these eddies is associated with the advection of warmer, fresher water masses from the
50 outflow of Hecate Strait. These buoyant water masses generate small anticyclonic eddies
51 west of Cape St. James. When the flow is strong, typically in the winter, several of these
52 small eddies can merge to form a larger Haida eddy. The center of the Haida eddy
53 generally includes mixed layer water from Hecate Strait, Queen Charlotte Sound, and the
54 continental shelf off northern Vancouver Island (Di Lorenzo *et al.*, 2005). For example,
55 Crawford (2002) noted that the temperature of Haida eddies in summer at 150 m depth
56 matched surface temperatures at Cape St. James in the preceding winter.

57 Sitka eddies were first described by Tabata (1982) and form near Baranof Island, Alaska
58 at approximately 57°N, 138°W. Model studies suggest that Sitka eddies are formed via
59 baroclinic instabilities in the northward flowing currents along the continental slope,

60 forced by Kelvin waves and southerly winter winds (Melsom *et al.*, 1999; Murray *et al.*,
61 2001). The formation location appears to be due to interactions with the local topography
62 (Swaters and Mysak, 1985).

63 Gower (1989) identified a third GOA eddy formation region near Yakutat, Alaska. The
64 shelf in this region is much wider (~100 km) than those near the Sitka and Haida eddy
65 formation regions. Yakutat eddies generally stay close to the shelf-break as they move
66 westward around the boundary of the GOA (Ladd *et al.*, 2005a). They have been
67 observed to carry excess heat, salinity, and nutrients in their subsurface core waters that
68 can be distinguished from the surrounding basin water at least a year after formation
69 (Ladd *et al.*, 2007).

70 Based on water properties, Favorite, *et al.*, (1976) describe the Dilute and the Ridge
71 Domains in the GOA. The Dilute Domain is indicated by salinity < 33.0 at 100m and
72 extends seaward from the coast of North America to roughly 160°W (Fig. 1). The Ridge
73 Domain, north of the Dilute Domain, is defined as the region of bowed up isopycnals
74 associated with the center of the Alaskan Gyre. Haida eddies form and stay in the Dilute
75 Domain, while Sitka and Yakutat eddies form in the broad Alaska Current, often
76 translating into the Ridge Domain.

77 Westward propagation of mesoscale eddies in deep-sea waters is attributed to planetary
78 beta effects, whereby the change in magnitude of Coriolis force with latitude pushes
79 eddies westward at all latitudes. Haida and Sitka eddies form where the continental
80 margin is oriented mainly NNW to SSE and propagate into deep-sea waters within

81 months of formation. Yakutat eddies form closer to the East-West oriented margin, and
82 stray little from this margin during their westward propagation.

83 Temperature inversions, with a temperature minimum above a deeper temperature
84 maximum, occur throughout the subarctic North Pacific Ocean (Roden, 1964; Uda,
85 1963). The temperature maximum and minimum have been called the mesothermal and
86 dichothermal waters, respectively (Uda, 1963). The warm and saline mesothermal water
87 is related to the circulation and ventilation of North Pacific Intermediate Water (Ueno
88 and Yasuda, 2001, 2003). However, formation processes contributing to temperature
89 inversions in the North Pacific have been found to vary regionally. Seasonal cooling of
90 the dichothermal layer as well as advection of heat and salinity into the mesothermal
91 layer have both been found to be of importance in maintaining the temperature inversion
92 structure (Musgrave *et al.*, 1992; Ueno *et al.*, 2007; Ueno and Yasuda, 2000, 2005). By
93 transporting excess heat and salinity into the basin (Ladd *et al.*, 2007), Yakutat eddies
94 may be important in the maintenance of mesothermal waters in the GOA (Onishi *et al.*,
95 2000; Ueno and Yasuda, 2005).

96 The central GOA is described as high nitrate – low chlorophyll (HNLC) and the role of
97 iron in controlling primary productivity has been widely accepted (Boyd *et al.*, 2004;
98 Boyd *et al.*, 1998; Martin *et al.*, 1989; Martin and Gordon, 1988). Eddies have been
99 suggested as one mechanism that may enhance cross-shelf exchange (Crawford and
100 Whitney, 1999; Ladd *et al.*, 2005b; Okkonen *et al.*, 2003; Stabeno *et al.*, 2004)
101 influencing nutrient limitation in the GOA. Haida eddies carry shelf-derived nutrients
102 (Whitney and Robert, 2002) and biota (Mackas and Galbraith, 2002) westward into the
103 basin. In the Haida eddy region, observations show low nitrate versus salinity at a coastal

104 upwelling station, high nitrate versus salinity in basin water (Ocean Station P, OSP;
105 50°N, 145°W), with eddy waters in between (Peterson *et al.*, 2005). In the first study of
106 iron transport via GOA eddies, Johnson *et al.* (2005) showed that young Haida eddies
107 contain dissolved iron concentrations almost two orders of magnitude higher than is
108 typically observed at OSP. In addition, 16 months after its formation, one Haida eddy
109 still contained 1.5 – 2 times more iron than surrounding water.

110 This paper reports on the first multidisciplinary set of observations of all three eddy types
111 (Haida, Sitka, and Yakutat) in a single year soon after their formation. Due to ongoing
112 observations along Line P, Haida eddies have been well sampled (e.g. Crawford, 2002;
113 Crawford *et al.*, 2002; Mackas and Galbraith, 2002; Whitney and Robert, 2002).

114 However, only a few directed eddy studies have been accomplished in the two northern
115 eddy types (Ladd *et al.*, 2005a; Ladd *et al.*, 2007) and they were accomplished in older
116 eddies (offshore of Kodiak Island in the western GOA). In addition, while one study has
117 examined iron concentrations in Haida eddies (Johnson *et al.*, 2005), the two northern
118 eddy types have not previously been sampled for iron.

119 **2. Methods**

120 The bulk of the data to be discussed here is from a research cruise (Fig. 1) on the R/V
121 *Thomas G. Thompson* in the spring of 2005 (April 26 – May 8). This cruise was a multi-
122 disciplinary, international investigation of the influence of eddies in the eastern Gulf of
123 Alaska. Three eddies were sampled (from south to north, Haida, Sitka, and Yakutat
124 eddies) for temperature and salinity, macro-nutrients, iron, chlorophyll and zooplankton
125 (as well as other data not discussed here). The emphasis of this paper will be on data from

126 the Haida transect (casts 1 – 16) and the long northward transect across the Sitka and
127 Yakutat eddies (casts 30 – 60). The east-west transect across the Sitka eddy (casts 18-29)
128 was primarily to deploy two drifters to more accurately estimate the location of the center
129 before intensive sampling. During this east-west transect, 12 CTD casts were made to
130 only 600m. These data will not be discussed further.

131 Additional data used to help characterize Alaska Gyre waters and evolution of eddies
132 were collected onboard the R/V *John P. Tully* in June 2005. Procedures were similar to
133 those used on the *Thompson* survey.

134 **2.1 CTD data**

135 A SeaBird 911 plus CTD was equipped with dual temperature and conductivity sensors, a
136 fluorometer, a SBE43 dissolved oxygen sensor, and a transmissometer. On each cast,
137 salinity, chlorophyll and nutrient samples were taken from Niskin bottles. Chlorophyll
138 samples were filtered through Osmonics glass fiber filters (nominal pore size 0.7 μm),
139 and stored in the dark at -80°C for several months before extracting in 90% acetone for
140 24 hours. Fluorometric determination of chlorophyll concentration (acidification method,
141 (Lorenzen, 1966)) was made using a Turner Designs TD700 fluorometer calibrated with
142 pure chlorophyll *a*. Nutrient samples were analyzed aboard ship (see section 2.2).
143 Salinity samples were taken on every cast to calibrate the CTD salinity measurements.

144 **2.2 Nutrient and oxygen sampling**

145 Water samples for dissolved inorganic nutrients (NO_3 plus NO_2 , PO_4 , and SiO_4) were
146 drawn from CTD rosette casts, GO-FLO casts, and the underway, uncontaminated

147 seawater supply into acid cleaned polycarbonate test tubes and stored up to 12 h before
148 being analyzed. All samples were analyzed onboard ship using a Technicon
149 AutoAnalyzer II following procedures in Barwell-Clarke and Whitney (1996). Since
150 NO_2 is a trivial portion of the NO_3 plus NO_2 analysis, these data will be subsequently
151 referred to as NO_3 or nitrate.

152 Nutrient samples were collected from the surface bottle of every CTD cast and from the
153 following sampling depths of approximately every other CTD cast: 0, 10, 20, 30, 40, 50,
154 60, 75, 100, 120, 150, 200, 250, 300, 400, 600, 800, 1000, 1250, 1500, 1750, and 2000
155 meters for a total of 680 samples. Nutrients were also sampled from 16 Go-Flo casts (see
156 section 2.3).

157 On the cruise in June 2005, oxygen samples were analyzed on an automated Winkler
158 titration system following the procedures of Carpenter (1965). A Brinkmann model 665
159 Dosimat and model PC910 Colorimeter is controlled by a Visual-Basic program to titrate
160 the oxygen samples.

161 **2.3 Iron data**

162 Iron is ubiquitous as a contaminant during sampling and analytical procedures making
163 accurate measurement extremely difficult. Thus, great care must be taken in all phases of
164 shipboard sampling, handling, and analysis. A detailed description of sampling and
165 analysis methodology is included in Johnson *et al.* (2005) and will not be repeated here.

166 Sampling was initiated on 28 April at a “reference” station (station 1; Fig. 1) in an area
167 with low surface chlorophyll concentrations according to concurrent satellite ocean color

168 data. Surface sampling was conducted away from the *Thompson* from the ship's
169 Zodiac/Hurricane rigid hull inflatable using wide mouth bottles (1 liter and 500ml).

170 The shallower depths of 10, 20, 30, and 40 m were sampled using an air driven, double
171 bellows, all plastic/Teflon Asti pump and Teflon lined PVC half inch ID tubing. These
172 samples were filtered in the on-deck HEPA hood in the staging bay. For greater depths
173 (50, 75, 100, 150, 200, 300, 400, 600, and 800 m), twelve liter General Oceanic (G.O.)
174 Go-Flos or X-Niskins were used and sub-sampled in the wet lab using bell jar dust covers
175 and 0.22u Opticap cartridge filters. As noted above, nutrient samples were also collected
176 from the Go-Flo sample bottles. All samples were processed inside a plastic clean tent
177 constructed in the ship's main lab. A class 100 HEPA filter maintained a clean
178 environment and positive pressure inside the tent for processing and handling reagents,
179 standards, and samples. Of the 4 sub-samples collected for iron, one filtered (dissolved)
180 and one unfiltered (labile) were analyzed onboard by FIA chemiluminescence in the
181 clean tent. The other two were acidified to pH 1.7 with 1 ml of 6N HCL per 125 ml
182 seawater for later analysis of total dissolved iron and total iron. In this paper, we only
183 discuss the labile and total iron concentrations.

184 Profile data (to 800 m) for iron and nutrients were collected for the reference station (cast
185 1), Haida eddy center (cast 10), Haida edge (cast 15), a reference station outside Dixon
186 Entrance (cast 17), Sitka eddy edge (cast 31), Sitka center (cast 39), and Yakutat eddy
187 center (cast 52) (Fig. 1; filled circles). All profiles were sampled identically except for
188 the Yakutat eddy center station, which did not have a surface iron sample. In addition to
189 the 800 m profiles, shallower samples were collected as follows. For the Haida eddy,
190 samples were collected from 10 and 40 m for three stations. For the Sitka eddy, samples

191 from 10 and 100m were collected at six stations on the east-west line (Fig. 1; grey filled
192 circles).

193 **2.4 Zooplankton Data**

194 Zooplankton samples were collected using paired bongo frames (60 and 20 cm diameter)
195 with 333 and 153 μm mesh nets, respectively. Nets were equipped with calibrated
196 flowmeters, a real-time depth sensor and were towed obliquely to about 10m off bottom
197 or 300 m whichever was shallower (Incze *et al.*, 1997). Samples were preserved in 5%
198 buffered Formalin, and were identified and sorted by the Polish Plankton Sorting and
199 Identification Center (ZSIOP) in Szczecin, Poland.

200 The software package Primer was used to perform the statistical analyses. The taxa rarely
201 encountered in the samples (occurring at $< 8\%$ of stations) were eliminated from the first
202 round of analyses, except for barnacle larvae which were included because of their
203 potential to identify water of nearshore origin. During a subsequent statistical analysis,
204 adult copepods from under-represented families that potentially had warm-temperate
205 origins were included.

206 **2.5 Drifter data**

207 Satellite-tracked drifter data were used to increase the precision of eddy center location
208 estimates in order to direct the *in situ* sampling, to estimate the location of the *in situ*
209 sampling relative to the eddy center, and to provide information regarding flow patterns,
210 speeds, and residence times in and around the eddies. A total of eight satellite-tracked
211 drifters (Table 1), drogued at 40 m with “holey sock” drogues, were deployed in the three

212 eddies. One drifter (53319) was deployed in the Haida eddy in early March. Two other
213 drifters (53309 and 53312) were deployed approximately one week prior to the
214 *Thompson* cruise. These three initial drifters helped locate the center of the Haida eddy
215 without the need for a preliminary transect. An additional drifter (53310) was deployed
216 at the estimated center location from the *Thompson*. Two drifters each were deployed in
217 the Sitka (53321 and 53308) and Haida (53304 and 53306) eddies resulting in a total of
218 five drifters deployed from the R/V *Thomas G. Thompson* (Table 1). Center locations
219 were calculated using data from one full circuit around the eddy bracketing the time
220 period of interest. The location of the center of the circuit was calculated as an average
221 of latitude and longitude over the full circuit.

222 **2.6 Satellite data**

223 Gridded sea surface height anomalies (SSHA) were downloaded from Aviso. The “ref
224 merged” dataset (obtained from <http://www.jason.oceanobs.com>) consists of delayed-
225 mode, merged data from two satellite missions, Jason-1 and Envisat. This dataset has
226 stable sampling in time (SSALTO/DUACS, 2006). The optimal interpolation
227 methodology used by Aviso to merge data from multiple altimeters is described by Le
228 Traon *et al.* (1998). The mapped altimetry data set includes one map every 7 days with a
229 $1/3^\circ$ spatial resolution on a Mercator grid (Ducet *et al.*, 2000; Le Traon and Dibarboure,
230 1999). Merging data from multiple satellites with differing spatial and temporal
231 resolution helps resolve the mesoscale allowing for a better description of eddy activity
232 (Ducet *et al.*, 2000; Le Traon and Dibarboure, 2004).

233 Science-quality chlorophyll-a concentration data at the ocean surface from MODIS on
234 the Aqua satellite (downloaded from <http://coastwatch.pfeg.noaa.gov>) are used to show
235 the spatial context within which our in situ observations were made. NASA's Goddard
236 Space Flight Center receives the raw satellite data. Processing is accomplished using the
237 SeaWiFS Data Analysis System (SeaDAS) software (Fu *et al.*, 1998). An atmospheric
238 correction is applied to the data to yield a measurement of water leaving radiance
239 (Gordon and Wang, 1994; Shettle and Fenn, 1979). These radiances are processed to
240 chlorophyll-a concentration using the NASA developed OC3M algorithm (described in
241 O'Reilly *et al.*, 2000). This algorithm is analogous to the OC4v4 algorithm used in the
242 processing of SeaWiFS data, but adjusted for the specific bands available on the MODIS
243 sensor. The chlorophyll-a data are best used for feature identification and tracking. The
244 actual value of the chlorophyll-a is somewhat controversial due to major differences
245 when compared to that of the SeaWiFS sensor on Orbview-2. Both can differ
246 substantially from high-quality in-situ measurements.

247 **3. Results**

248 **3.1 Formation and translation**

249 Anticyclonic eddies have a positive SSHa signature. Thus altimetric SSHa were used to
250 track the formation of the eddies before the cruise. The Sitka eddy appeared first around
251 15 December 2004, followed almost a month later (12 January 2005) by the Haida eddy
252 (Fig. 2; note that the dates shown are slightly later than the first evidence of the eddies in
253 order to show the eddies at sufficient strength). The Yakutat eddy was first observed off-

254 shelf in the altimetry record on 16 March 2005. However, positive SSH anomalies were
255 present on the relatively wide shelf near Yakutat for two weeks prior, providing evidence
256 for formation on the shelf. The Yakutat eddy was the youngest, at only 1.5 months, of
257 the three eddies sampled (Table 2). While the Sitka and Haida eddies first appeared in
258 the altimetry record in deep water off the narrow continental shelves of their formation
259 regions, altimetry data provided evidence that the Yakutat eddy formed on the wider shelf
260 north of Cross Sound and subsequently translated into deeper water.

261 The Haida eddy was sampled from 28 April to 1 May 2005, when the eddy was ~3.5
262 months old. The center station (cast 10; 52.33°N, 133.29°W) was occupied on 30 April
263 2005. As noted in section 2.5, the deployment of drifters in the eddy allowed a precise
264 estimate of the location of the center of the eddy prior to conducting the transect. The
265 location of the center of the eddy derived from drifter trajectories was 52.35°N,
266 133.30°W, a distance of < 3 km from cast 10. The Haida eddy continued to drift slowly
267 toward the northwest, disappearing from the altimetry record in January 2006. During
268 this time, the eddy moved less than 300 km from where it was sampled.

269 Drifters were not deployed in the Sitka or Yakutat eddies prior to the cruise. Prior to
270 sampling these eddies, the center location of the Sitka eddy was estimated from altimetry
271 and ocean color data. The ship conducted a transect from east of the Sitka eddy toward
272 the southwest to deploy two drifters to more accurately estimate the location of the center
273 before intensive sampling. By the time the ship was on location at the southern end of
274 the northward transect across the two eddies, data from the two drifters allowed a more
275 precise estimate of the center location of the Sitka eddy. The center of the Sitka eddy

276 was sampled (cast 39) on 5 May 2005 at a distance of < 3 km from the center derived
277 from drifter measurements.

278 Due to time constraints, a cross-section of the Yakutat eddy was not possible prior to
279 intensive sampling. Based on drifter data from drifters deployed during the ship's only
280 transect, the center of the Yakutat eddy was 57.90°N, 139.85°W. The closest CTD cast
281 (cast 51) was ~7 km away while the nearest nutrient and iron data were sampled at cast
282 52, ~13 km from the center.

283 During sampling, the centers of the Sitka and Yakutat eddies were only 114 km apart.
284 The radius of the Sitka eddy was ~ 40 km, based on where the isopycnal slope changed
285 sign, while the radius of the Yakutat eddy was ~ 75 km. Both the Sitka and the Yakutat
286 eddies retained their respective two drifters until ~15 June 2005 when the eddies merged.
287 At this point, the four drifters began circling one larger merged eddy. Two of the drifters
288 stayed with the merged eddy until mid-November 2005 when they both exited the eddy
289 almost simultaneously.

290 **3.2 Temperature and Salinity**

291 The temperature and salinity observed in the three eddies (Fig. 3) reflect the different
292 domains in which they form. Below the mixed layer, the Haida eddy exhibits warmer
293 and saltier water than the two more northern eddies (Table 3) reflecting its more southern
294 location and the greater influence of subtropical waters (see section 3.4).

295 The Sitka and Yakutat eddies both exhibited a temperature inversion (Figs. 3 and 9). A
296 similar inversion was observed at the center of the 2003 Yakutat eddy observed in the

297 western GOA (Ladd *et al.*, 2005a). The temperature minimum ($T_{\min} < 6.5^{\circ}\text{C}$) occurred at
298 depths of approximately 50 – 100 m, while the temperature maximum ($T_{\max} > 6.5$)
299 occurred from 125 – 250 m depth. High levels of iron were coincident with the
300 mesothermal (T_{\max}) water (discussed further in section 3.5). The difference in
301 temperature $\Delta T = T_{\max} - T_{\min}$ was $\sim 0.5^{\circ}\text{C}$ at both the center of the Sitka eddy and the
302 center of the Yakutat eddy. The water properties of the T_{\min} and T_{\max} within the Sitka
303 and Yakutat eddies are consistent with those found by (Ueno and Yasuda, 2005) for the
304 eastern Gulf of Alaska. Tabata (1982) notes temperature inversions frequently occur in
305 Sitka eddies. Conversely, the Haida eddy exhibited no temperature inversion, consistent
306 with findings that inversions are infrequent in the area east of 140°W and south of 54°N
307 (Ueno and Yasuda, 2005), although Crawford (2002) notes small temperature inversions
308 in the five Haida eddies he examined. We believe that Haida eddies themselves create
309 subsurface temperature maxima near 150 m depth as they propagate westward and
310 southwestward through increasingly cooler and saltier subsurface waters of the mid-
311 Alaska Gyre.

312 The freshest water sampled (31.7) occurred on the southern edge of the Sitka eddy (cast
313 34) (Fig. 3). MODIS chlorophyll data shows a ribbon of high chlorophyll being pulled
314 away from the shelf and wrapped around the eddy (Fig. 4). The transect through the
315 Sitka eddy crossed this ribbon of high chlorophyll near cast 34. In fact, the highest 10 m
316 chlorophyll concentrations measured on the cruise were observed at cast 34. This
317 suggests that the circulation of the eddy may have actively pulled coastal water, with its
318 low salinity and high chlorophyll, off the shelf and into the basin. Similar advection of
319 coastal chlorophyll off-shelf has been observed in other GOA eddies (Crawford *et al.*,

320 2005; Crawford *et al.*, 2007; Ladd *et al.*, 2005a; Okkonen *et al.*, 2003). Other than this
321 ribbon of low salinity, the lowest salinity sampled during the transects occurred at the
322 surface in the center of the Yakutat eddy (Table 3). This may be due to the surmised on-
323 shelf formation location (trapping fresher coastal water in the center of the Yakutat eddy)
324 or due to the fact that the Yakutat eddy was the youngest of the three eddies and the
325 coastal signature at the center of the eddy had not yet had time to mix away.

326 Surface mixed layer depth (defined as the depth where σ_θ is 0.125 denser than the
327 surface) in the Haida eddy was deeper (~50 m) than in the Sitka and Yakutat eddies (5 –
328 10 m). The comparison of mixed layer depths illustrates the dangers of assuming
329 synopticity in a study such as this. The differences in mixed layer depth were probably at
330 least partly due to differences in atmospheric forcing prior to sampling each of the eddies.
331 During the three days prior to sampling the Haida eddy (28 Apr – 30 Apr 2005), wind
332 speed measured by the ship averaged 7.8 m s^{-1} and shortwave radiation averaged 152 W
333 m^{-2} . During the three days prior to sampling the Sitka eddy (3 May – 5 May 2005), wind
334 speed and shortwave radiation averaged 2.5 m s^{-1} and 217 W m^{-2} respectively. The 30%
335 decrease in wind speed and over 40% increase in solar radiation during that time period
336 likely contributed to the shallower mixed layer observed in the northern eddies. The
337 proximity of the eddies to fresh water sources during formation likely also influenced the
338 depth of the surface mixed layer.

339 **3.3 Macronutrients**

340 Nitrate in the surface 50m of the Haida eddy was between 5 and $10 \mu\text{M}$, except at the
341 center of the eddy where bowed-up, near-surface isopycnals were associated with slightly

342 higher nitrate concentrations (11.7 μM) at 45m (Fig. 5). Nitrate averaged 10.4 μM over
343 the 56m deep mixed layer in the center of the Haida eddy (Table 3). Nitrate in the mixed
344 layer of the 2005 Haida eddy was lower than that measured in a Haida eddy in February
345 2000 but higher than the same eddy sampled in June 2000 (Peterson *et al.*, 2005).
346 Assuming similar nitrate values in different Haida eddies suggests that nutrient
347 drawdown had already begun when the 2005 Haida eddy was sampled. A weak
348 chlorophyll maximum was observed 20 – 40 km from the center of the eddy at ~10 m
349 depth.

350 The Sitka eddy had depleted nitrate in the surface waters at ~40 – 60 km from the center
351 (casts 34, 35, 45, and 46) indicating that a bloom had already occurred. Below these
352 depleted waters, a subsurface chlorophyll maximum was observed at 10 – 20m depth
353 where nitrate was ~5 – 10 μM . As mentioned in section 3.2, cast 34 had the lowest
354 salinity and highest 10 m chlorophyll measured on this cruise. The surface mixed layer at
355 the center of the Sitka eddy was also lower in nitrate (and silicic acid and phosphate) and
356 higher in chlorophyll than in the other two eddies (Table 3).

357 The mixed layer of the Yakutat eddy exhibited lower chlorophyll than the Sitka eddy
358 along with higher nitrate and iron than both the Sitka and Haida eddies (Table 3). With
359 the exception of the casts at the center of the Yakutat eddy (casts 47 – 54), the silicic acid
360 versus nitrate relationship (Fig. 6) exhibits a strong linear regression ($S = 1.3N + 2.9$; $R^2 =$
361 0.95). Silicic acid appears to be slightly higher per unit nitrate in the Sitka/Yakutat
362 transect than in the Haida transect. This may be due to the higher influence of California
363 Undercurrent water (discussed further in section 3.4) on the Haida eddy core waters
364 (Whitney *et al.*, 2005; Whitney and Welch, 2002). At the center of the Yakutat eddy,

365 silicic acid values in the top 100 m were relatively constant ($22 \mu\text{M} < \text{silicic acid} < 35$
366 μM) and did not conform to the regression equation (Fig. 6). (Phosphate versus nitrate
367 had a tight relationship in all of the eddies; $N=16.6P - 8.6$; $R^2 = 0.98$). High silicate
368 concentrations in low salinity waters indicate riverine inputs to the core waters of the
369 eddy (Whitney *et al.*, 2005). It is unclear why the Sitka eddy would have high
370 chlorophyll concentrations and nutrient drawdown while the Yakutat eddy is low in
371 chlorophyll but has plenty of nutrients. It is possible Yakutat surface waters had recently
372 upwelled from below the euphotic layer, pushing aside surface waters previously at the
373 center. This eddy also formed 2 months later than the Sitka and Haida eddies, allowing
374 less time for favorable phytoplankton growth conditions to occur.

375 Below the mixed layer, nitrate versus salinity was generally higher in the Sitka/Yakutat
376 transect than in the Haida transect (Fig. 7), possibly due to large scale differences
377 between the Dilute Domain and the Alaska Gyre Domain. (The depth and density ranges
378 of the subsurface core waters in each eddy are noted in Table 3.) In the subsurface core
379 waters ($32.4 < S < 33.8$), the highest nitrate per unit salinity measured in the entire
380 dataset was at the center of the Sitka eddy. The centers of the Yakutat and the Haida
381 eddies showed levels of nitrate per salinity similar to each other in the subsurface core.
382 These levels were also similar to those observed in a 5-month-old Yakutat eddy in spring
383 2003 (Ladd *et al.*, 2005a), but 10 – 20% higher nitrate per salinity than observed in the
384 2000 Haida eddy (Peterson *et al.*, 2005). Except in the surface waters ($S < 32.2$), the
385 center of the Yakutat eddy was not particularly anomalous compared to other data
386 collected on the Sitka/Yakutat transect. On the other hand, the nitrate versus salinity at
387 the center of the Haida eddy was much higher than other observations on the Haida

388 transect. Data from the Haida reference station had the lowest nitrate per unit salinity
389 indicating that this station consisted of coastal water (Peterson *et al.*, 2005). Patterns of
390 surface chlorophyll (Fig. 4) show high chlorophyll wrapped around the edges of the
391 Haida eddy supporting this conclusion. Patterns of silicic acid and phosphate –salinity
392 relationships were similar (not shown).

393 **3.4 Oxygen and NO**

394 Oxygen enters the subsurface waters of the subarctic Pacific in ventilation sites along the
395 Asian coast (Whitney *et al.*, 2007). As these waters flow across the Pacific in isolation
396 from the atmosphere, remineralization consumes oxygen and produces nitrate. Oceanic
397 waters in the Alaska Gyre exhibited higher oxygen levels than those of either the three
398 eddies or the shelf waters of Queen Charlotte Sound, especially in the eddy core water
399 density range ($\sigma_\theta \sim 25.4$ to 26.8) (Fig. 8b). Low coastal oxygen levels are the result of
400 longer isolation from the atmosphere, shelf remineralization processes and the northward
401 transport of subtropical waters via the California Undercurrent (Whitney *et al.*, 2007;
402 Whitney *et al.*, 2005). In the eddy core waters, oxygen was slightly higher in the
403 northern eddies than in the Haida eddy. Haida 2005 showed consistent levels of oxygen
404 between the April and June sampling periods. Nitrate, on the other hand, decreased in the
405 Haida eddy from April to June (Fig. 8a). However, in April, nitrate at cast 8 (~10 km
406 from the center cast) was less than nitrate at cast 9 (center) by an amount similar to the
407 difference between April and June. This suggests that the observed decrease between
408 April and June could be explained by slightly different sampling location within the eddy.
409 The reference station (cast 1) shows a fairly strong coastal influence (lower oxygen)

410 compared with OSP. The spike in oxygen at a density of 26.7 at OSP suggests a
411 ventilation event propagating from the Asian coast into the Alaska Gyre. Oxygen
412 replenishment in the NE Pacific depends on such periodic events (Whitney *et al.*, 2007).

413 Broecker (1974) derived a conservative tracer ($\text{NO} = \text{O}_2 + 9\text{NO}_3$) based on the preformed
414 levels of nitrate and oxygen in a watermass. Watermasses formed in cold regions with
415 high nitrate levels will have high NO while waters formed in warmer regions with low
416 nitrate will carry a low NO signature. As these waters sink and no longer exchange gases
417 with the atmosphere, remineralization of organic matter consumes oxygen and produces
418 nitrate in a fairly constant ratio as long as oxygen is available. The ratio of oxygen
419 consumption to nitrate production (9.2) is persistent in the interior waters of the Alaska
420 Gyre (Whitney *et al.*, 2007). Thus, following Whitney *et al.* (2007), we use a slightly
421 modified tracer: $\text{NO} = \text{O}_2 + 9.2\text{NO}_3$. Strong regional differences in NO have been
422 observed throughout the North Pacific with minima in the subtropics and in the
423 California Undercurrent (CUC) (Whitney *et al.*, 2007). Low NO in the CUC is the result
424 of denitrification along the Central American and California coasts (Castro *et al.*, 2001).

425 NO of slope waters is low in our study region (Fig. 8c; Queen Charlotte Sound)
426 indicating that the dominant source of this water must be the CUC. Using data from
427 Whitney *et al.* (2007), we estimate the slope and Haida eddy waters on the 26.7 isopycnal
428 to be 85% subtropical in April 2005, based on Alaska Gyre and CUC values of 450 and
429 $380 \mu\text{mol NO kg}^{-1}$ respectively. Relatively low NO of CUC origin is found also in each
430 of the eddies at densities greater than ~ 25.8 . However, this southern influence is weaker
431 (higher NO) in the Sitka and Yakutat eddies than in the Haida eddy. The NO of the
432 eddies and the reference stations is fairly constant between 26.4 and 26.8 σ_θ . The Haida

433 eddy in both April and June had values of $390 \mu\text{mol kg}^{-1}$, the same as the slope station in
434 Queen Charlotte Sound. Both Sitka and Yakutat core waters were $400 \mu\text{mol kg}^{-1}$,
435 compared with $405 \mu\text{mol kg}^{-1}$ for the Haida reference station and 450 for OSP. Since
436 these differences reflect the contribution to eddies from the subtropics and the Alaska
437 Gyre, they may help explain differences in plankton communities found within them (see
438 Section 3.6).

439 **3.5 Iron**

440 Labile iron at the Haida reference station averaged 0.10 nM in the mixed layer, increasing
441 to a maximum of 1.24 nM at 600 m depth. While the mixed layer values are typical of
442 Alaskan Gyre (i.e. OSP) waters, the deeper values are much higher than typically
443 observed in the open Alaskan Gyre (Johnson *et al.*, 2005) supporting the above
444 conclusion (based on nitrate versus salinity values) that the reference station consisted of
445 coastal water that had advected around the outside of the eddy. However, these values
446 are significantly lower than those measured at the center of the eddies or in an actively
447 forming eddy off the southern Queen Charlotte Islands in February 2001 (Johnson *et al.*,
448 2005). These differences may indicate that the source of the reference station water is not
449 Hecate Strait (the likely source of Haida eddy core water). Maximum iron (both labile
450 and total) at the center of the Haida eddy occurred at 200 m . The zone of elevated iron
451 (with labile iron levels typical of coastal waters; (Johnson *et al.*, 2005)) extended to ~ 550
452 m and $\sigma_{\theta} \sim 26.8$ (Fig. 9), the typical depth of Haida eddy core water (Whitney and
453 Robert, 2002). Four-month-old Haida eddies were sampled in June 2000 and June 2001
454 (Johnson *et al.*, 2005). The centers of these two eddies had labile and total iron profiles

455 that were very similar to each other (labile ~ 2 nM; total ~ 5 nM at 200 m). The labile
456 and total iron concentrations in the core waters of the 2005 Haida eddy (Table 3) were
457 two to three times the concentrations measured in the 4-month-old 2000 and 2001 Haida
458 eddies. Altimetry data suggests that the 2001 eddy was weak (SSHA ~ 4 cm in June
459 2001) while the 2000 and 2005 Haida eddies were much stronger (SSHA ~ 21 cm in June
460 2000 and ~ 17 cm in May 2005). The 2005 eddy was sampled approximately one month
461 earlier in the spring than the 2000 and 2001 eddies, suggesting that the spring bloom had
462 not had as much time to draw down the iron concentrations before our sampling in 2005.
463 Interannual variability in the iron concentration of the source waters may also contribute
464 to the differences between eddies.

465 While lower than those measured at the center of the Haida eddy, the iron concentrations
466 in the center of the Sitka eddy (Table 3) were still typical of coastal rather than open
467 basin waters. The vertical distribution, with elevated levels (relative to outside waters) to
468 about 550 m ($\sigma_\theta \sim 26.8$), was similar to the Haida eddy indicating a core water depth of
469 ~550 m (Fig. 9). The highest total iron concentration measured on the cruise (> 60 nM;
470 too high for our measurement techniques), was found at the eastern edge of the Sitka
471 eddy at 100 m. Labile iron at this location was 5.81 nM at 100 m and 1.07 nM at 10 m.
472 Unfortunately, we only have iron measurements from 10 m and 100 m at this station.
473 This station may have been in the path of a tongue of coastal water that was being drawn
474 offshore. The high chlorophyll associated with this tongue can be seen in MODIS data
475 (Fig. 4) and appears to have originated from the shelf off of Baranof Island.

476 Other than this one station, the highest levels of iron were measured at the center of the
477 Yakutat eddy (Table 3) at 200 m. The total iron concentration at 200 m depth at the

478 center of the Yakutat eddy was more than twice as high as the maximum iron measured at
479 the center of the other two eddies (Fig. 9). The sharp peak in iron concentration of 41.4
480 nM at 200 m may reflect a source of iron from the sediments in the eddy formation
481 region. If this is true, it would suggest that the source of the eddy core water was
482 approximately 200 m deep. In contrast, the high iron concentration in the core of the
483 Sitka and Haida eddies was more broadly distributed over a deeper depth range,
484 reflecting the deeper (off-shelf) formation regions for these two eddies. Note that while
485 the depth range of the Yakutat eddy core waters was about half the depth range of the
486 other two eddies, the density range was similar (Fig. 9 and Table 3).

487 The peak in iron concentration (for both the Yakutat and Sitka eddies) is at the same
488 depth as the subsurface temperature maximum (T_{\max}). The coincidence of the high iron
489 coastal water signature with the T_{\max} suggests that the source of the temperature
490 maximum is coastal, lending support to suggestions (Onishi *et al.*, 2000; Ueno and
491 Yasuda, 2005) that eddies may contribute to the formation of temperature inversions
492 observed in the GOA.

493 **3.6 Zooplankton**

494

495 Zooplankton data were analyzed to examine differences between eddy center and edge
496 stations and differences between the three different eddies. There was no statistically
497 significant difference detected ($P = 0.659$) in zooplankton assemblages between edge and
498 center stations when data from all eddies were pooled. There was a statistically
499 significant difference between the zooplankton assemblages in the Haida and Sitka eddies
500 ($P = 0.008$), but not the Sitka and Yakutat ($P = 0.301$) or Yakutat and Haida eddies ($P =$

501 0.188), as determined by ANOSIM tests (analysis of similarity). A series of pairwise
502 SIMPER tests (similarity percentages) was conducted to learn which species were
503 contributing to the difference. ANOSIM and SIMPER tests are multivariate,
504 nonparametric permutation procedures used in ecology research (Clarke, 1993). In
505 general, the difference was due to higher abundances of members of the assemblage in
506 the Sitka eddy than in the Haida eddy, not to the presence or absence of particular taxa in
507 one or the other eddy. Sometimes the differences in abundance were on the order of 10 –
508 100 fold (Table 4). The notable differences in abundance between the two eddies were
509 for the groups: euphausiid developmental stages, larvaceans and several taxa of copepods
510 (*Acartia* spp., *Oithona* spp., *Neocalanus* spp.). Thecosomata (pteropods) were more
511 abundant in the Haida eddy than in the Sitka eddy.

512 **4. Discussion**

513 This paper presents the first directed observations in young Sitka and Yakutat eddies near
514 their formation regions, whereas Haida eddies have been well studied through their
515 evolution (e.g. Crawford, 2002; Johnson *et al.*, 2005; Whitney and Robert, 2002).

516 Previous published work on Sitka and Yakutat eddies has examined historical data for
517 evidence of eddies (Tabata, 1982) or examined older eddies near Kodiak Island in the
518 northwestern GOA (Ladd *et al.*, 2005a; Ladd *et al.*, 2007). Synoptic sampling shows that
519 the temperature and salinity of the Sitka and Yakutat eddy core waters were very similar
520 to each other and colder than the Haida eddy. This is not surprising in that the Sitka and
521 Yakutat eddies were close together (centers ~115 km apart) and form farther north where
522 the influence of the California Undercurrent is weaker. Additionally, the T/S properties

523 in the cores of these eddies are not significantly different from the surrounding waters
524 outside the eddies. However, Ladd *et al.* (2007) showed that after leaving the eastern
525 GOA, these eddies carry anomalous heat and salt along constant σ_θ surfaces into the
526 western GOA.

527 The nutrient signatures of all three eddies were quite different from each other,
528 suggesting differing biological activity and/or differing formation regions and source
529 waters. The 2005 Yakutat eddy had significantly higher nutrient content (including iron)
530 in the surface waters than the Sitka and Haida eddies (Table 3). High silicic acid and low
531 salinity suggests that the source of the Yakutat eddy surface waters is strongly influenced
532 by river runoff (Whitney *et al.*, 2005). Unfortunately, little winter data from this shelf
533 region exists with which to compare.

534 While iron in Haida eddies has been previously sampled (Johnson *et al.*, 2005), the
535 current work presents the first observations showing that the Sitka and Yakutat eddies
536 also supply excess iron to the basin. In fact, iron concentrations measured in the Yakutat
537 eddy were higher than any previous Haida eddy measurements (Johnson *et al.*, 2005),
538 including measurements from a forming eddy where biological drawdown had
539 presumably not yet occurred. In the surface mixed layer, the Yakutat eddy exhibited
540 twice as much iron (both total and labile) as that measured in the Haida eddy (Table 3),
541 probably because the spring bloom had not yet utilized this nutrient. Integrated iron
542 values of excess eddy iron (calculated as the amount greater than the reference station)
543 were similar in the Haida and Yakutat eddies. Perhaps shelf iron in the Haida eddy was
544 initially found in a more concentrated shallow layer, but iron was scavenged and
545 distributed to greater depth following spring phytoplankton growth.. The Sitka eddy, on

546 the other hand exhibited less iron than the other two eddies. The center of the Yakutat
547 eddy appeared to be pre-bloom, with plenty of nutrients and iron in the surface layer and
548 relatively little chlorophyll. This may account for the high iron values in the surface
549 waters while iron in the surface waters of the other two eddies had already been utilized
550 by the bloom. The deeper core waters of the Yakutat eddy were also significantly higher
551 in iron than the Sitka and Haida eddies, possibly due to the shallow formation region and
552 the influence of iron input from the sediments. The iron maximum at 200 m and $\sigma_{\theta} \sim$
553 26.0 suggests eddy formation in approximately 200 m deep water with bottom densities
554 of $\sigma_{\theta} \sim 26.0$. Thus eddies formed on the shelf north of Cross Sound may be quite
555 important to providing iron to the GOA basin.

556 Our ability to detect real differences between the zooplankton assemblages from the
557 center and edge of eddies may have been hampered by our low number of samples, and
558 the inherent variability in the composition and abundance of species. Real differences
559 may have existed, but our sampling was inadequate to detect them.

560 We anticipated detecting differences between the zooplankton assemblages in the Haida
561 and Yakutat and the Sitka and Yakutat eddies. The Yakutat eddies form over shallow
562 water with substantial riverine input, and we expected to see a higher abundance of
563 species groups indicative of that water source. Marine cladocera, often associated with
564 nearshore water (Cooney, 1976), were absent from all the samples analyzed. Barnacle
565 larvae can also be an indicator of nearshore water, but they were only present at two
566 stations at this time of year (one in the Sitka eddy and one in the Haida eddy) and were in
567 relatively low abundance.

568 It is interesting that we detected a significant difference between the zooplankton
569 assemblages of the Haida and Sitka eddies. Both of these eddies form over deep water
570 and were similar in age. The main difference we found in the zooplankton was that the
571 abundances of several zooplankton groups were much higher in the Sitka eddy than in the
572 Haida eddy. Samples obtained from the Sitka eddy were assumed to be “post bloom” as
573 indicated by chlorophyll a and nutrient concentrations, while water samples from the
574 Haida eddy contained measurable nitrate and an average chlorophyll a value of 0.29 μg
575 liter⁻¹ in the surface mixed layer. It could not be determined from this sampling whether
576 or not the production and zooplankton abundance in the eddies was determined by
577 founder effects, bottom up or top down processes.

578 The taxa that accounted for most of the difference between the zooplankton assemblages
579 in the Sitka and Haida eddies are common groups, encountered frequently throughout the
580 study area. Zooplankton communities in Gulf of Alaska eddies are usually made up of a
581 mixture of oceanic and coastal species (Mackas and Galbraith, 2002), however our
582 sample analyses (i.e. the number and type of taxa identified to species) may have been
583 insufficient to detect the existing differences. Most of the zooplankton taxa accounting
584 for the statistical difference between the Haida and Sitka eddies were not identified to
585 species (euphausiid developmental stages, thecosomata, larvaceans, *Oithona* spp. and
586 *Acartia* spp.), only to general taxonomic group. These groups contain both oceanic and
587 coastal species (Mackas *et al.*, 2005). For example *Acartia longiremis* has been used as
588 an indicator of coastal water influence in Gulf of Alaska eddies (Batten and Crawford,
589 2005; Mackas and Galbraith, 2002). The adult *Acartia* spp. found in our samples would
590 need to be identified to species to see if the species composition of this group indicated

591 water mass origin. Other species considered to indicate coastal water were not found in
592 high abundances in either eddy (e.g. *Calanus marshallae*, (Mackas and Galbraith, 2002))
593 (Table 4). Our *Neocalanus* spp. group (*Neocalanus plumchrus* and *Neocalanus*
594 *flemingeri*), are known as part of the oceanic species complex common in Gulf of Alaska
595 eddies (Mackas and Galbraith, 2002), but are also common in coastal fjords such as the
596 Straits of Georgia and Prince William Sound, Alaska (Coyle and Pinchuk, 2005).

597 The Haida eddy exhibited greater influence of subtropical California Undercurrent water
598 than the two northern eddies as indicated by differences in NO concentrations. However,
599 zooplankton communities did not reflect this difference. The subtropical species groups
600 *Paracalanus* spp., *Mesocalanus tenuicornis* and *Pleuromamma* spp. (Gardner and Szabo,
601 1982; Mackas and Galbraith, 2002) were present at a few stations, but in extremely low
602 abundances and did not appear to be restricted to the Haida eddy. The copepod species
603 *Eucalanus bungii*, *Calanus pacificus* and *Metridia pacifica/lucens*, characterized as
604 subarctic by Mackas *et al.* (2005), were present in both Sitka and Haida eddies (Table 4).
605 *Calanus pacificus* had an extremely low abundance in both eddies, but was slightly more
606 abundant in the Haida eddy. *Eucalanus bungii* was in low abundance in both eddies
607 (average concentration: Haida 5.78 m⁻³; Sitka 13.69 m⁻³), but was more abundant in the
608 Sitka eddy. *Metridia pacifica/lucens* was in moderate abundance in both eddies, but was
609 also more abundant in the Sitka eddy. *Calanus pacificus*, *Eucalanus bungii* and *Metridia*
610 *pacifica/lucens* contributed just less than 10% to the dissimilarity of the zooplankton
611 assemblages in the two eddies (Haida and Sitka) (Table 4). It is unclear if the higher
612 abundance of these two subarctic species is an indication of an increased subarctic water

613 influence in the Sitka eddy, or just an artifact of the Sitka eddy's higher average
614 zooplankton abundance.

615 The coincidence of T_{\max} water with the high iron core water of the Sitka and Yakutat
616 eddies has interesting implications. By providing a source of T_{\max} water, these eddies
617 may contribute to the formation of temperature inversions in the GOA. Because iron is
618 so difficult to measure, the coincidence of T_{\max} water with high iron (if it holds up
619 throughout the region) could give information regarding the distribution (vertical and
620 horizontal) of high iron waters in the GOA. Using Argo profiling float data, Ueno *et al.*
621 (2007) examined distribution and interannual variability of temperature inversions in the
622 North Pacific. They found that, in the northern GOA, the T_{\min} water overlying the T_{\max}
623 outcropped in 2002 and 2004 but not in 2003. If winter mixing is deep enough to
624 ventilate the T_{\max} layer and its associated high iron, the iron can be mixed to the euphotic
625 zone resulting in higher iron availability to phytoplankton. Thus, interannual variability
626 of ventilation may influence iron sources to the surface waters. In addition, interannual
627 variability in eddy formation and pathways (Crawford *et al.*, 2007; Henson and Thomas,
628 2008; Ladd, 2007) suggests that iron input to the GOA via eddies may have strong
629 interannual variability which could influence productivity. Modeling studies show that
630 the formation and magnitude of eddies in the eastern GOA are forced by wind anomalies
631 associated with El Niño/Southern Oscillation and Pacific Decadal Oscillation cycles
632 (Combes and Di Lorenzo, 2007; Melsom *et al.*, 1999). Thus, eastern GOA eddies and
633 their associated iron transport may provide a link between indices of large scale climate
634 variability and productivity in the GOA.

635 Satellite data (chlorophyll and SSHA) support the *in situ* evidence that the Sitka eddy
636 forms in deeper water while the Yakutat eddy forms on the wider shelf north of Cross
637 Sound (Fig. 2). Source waters for the two eddies appear to be different, with coastal
638 water from Chatham Strait (south of Baranof Island) influencing the Sitka eddy while
639 water from Cross Sound and the shelf north of Cross Sound influences the Yakutat eddy.
640 NO suggests that the subsurface core waters of all three eddies (but especially the Haida
641 eddy) are also influenced by waters of subtropical origin via the California Undercurrent.

642 All three eddies had anomalously high levels of macronutrients and iron in their core
643 waters compared with surrounding basin waters. Additionally, satellite ocean color data
644 show all three eddies pulling streamers of coastal chlorophyll off-shelf while they were
645 close to the shelf-break. Properties of the Yakutat eddy are consistent with an on-shelf
646 formation in relatively shallow water (~200 m) while Haida and Sitka eddies appear to
647 form in deeper water (~600 m). The on-shelf formation and influence from the sediments
648 may account for the high levels of iron in the core of the Yakutat eddy while river input
649 at the surface may account for the high levels of silicic acid. Because this is the first
650 study of Sitka and Yakutat eddies near their formation region, it is unclear how typical
651 these properties might be.

652 ***Acknowledgements***

653 We are grateful to the captain and crew of the *R/V Thomas G. Thompson* for their
654 assistance in obtaining this dataset and to Calvin Mordy for discussions. Marie Robert
655 kindly provided Line P data. Peter Proctor and Janet Barwell-Clarke analyzed nutrient
656 samples. Nes Sutherland helped analyze iron samples. MODIS chlorophyll data were

657 obtained from NOAA CoastWatch Program and NASA's Goddard Space Flight Center,
658 OceanColor Web. The “ref merged” altimeter products were produced by Ssalto/Duacs
659 and distributed by Aviso with support from CNES. Near-real-time altimetry data from
660 the Colorado Center for Astrodynamics Research (CCAR) at the University of Colorado
661 helped in determining the location of the eddies during the research cruise. Thank you to
662 Kathryn Mier for providing the statistical analyses of the zooplankton data and to Jeffrey
663 Napp for improving the zooplankton discussions through his careful editing. Thank you
664 to Marc Trudel and the Canadian Coast Guard Ships *W.E. Ricker* and *Gordon Reid* for
665 deploying drifters in the Haida eddy prior to our cruise. The software used to calculate
666 the nutrient data was developed by David Jones, Department of Oceanography,
667 University of B.C., Vancouver. Canadian financial support was provided by Ocean
668 Sciences Division of Fisheries and Oceans Canada. This publication is partially funded
669 by the Joint Institute for the Study of the Atmosphere and Ocean (JISAO) under NOAA
670 Cooperative Agreement No. NA17RJ1232, Contribution #1476. This is contribution
671 #XXX to the U.S. GLOBEC program, jointly funded by the National Science Foundation
672 and National Oceanic and Atmospheric Administration, and PMEL contribution #3085.
673 This research is contribution EcoFOCI-G635 to NOAA's Fisheries-Oceanography
674 Coordinated Investigations.

675 **References**

- 676 Barwell-Clarke, J., Whitney, F., 1996. Institute of Ocean Sciences Nutrient Methods and
677 Analysis. Can. Tech. Rep. Hydrogr. Ocean Sci. 182, vi + 43 p.
- 678 Batten, S.D., Crawford, W.R., 2005. The influence of coastal origin eddies on oceanic
679 plankton distributions in the eastern Gulf of Alaska. Deep Sea Research Part II:
680 Topical Studies in Oceanography 52 (7-8), 991-1009.
- 681 Boyd, P.W., Law, C.S., Wong, C.S., Nojiri, Y., Tsuda, A., Levasseur, M., Takeda, S.,
682 Rivkin, R., Harrison, P.J., Strzepek, R., Gower, J., McKay, R.M., Abraham, E.,
683 Arychuk, M., Barwell-Clarke, J., Crawford, W., Crawford, D., Hale, M., Harada,
684 K., Johnson, K., Kiyosawa, H., Kudo, I., Marchetti, A., Miller, W., Needoba, J.,
685 Nishioka, J., Ogawa, H., Page, J., Robert, M., Saito, H., Sastri, A., Sherry, N.,
686 Soutar, T., Sutherland, N., Taira, Y., Whitney, F., Wong, S.-K.E., Yoshimura, T.,
687 2004. The decline and fate of an iron-induced subarctic phytoplankton bloom.
688 Nature 428 (6982), 549-553.
- 689 Boyd, P.W., Wong, C.S., Merrill, J., Whitney, F., Snow, J., Harrison, P.J., Gower, J.,
690 1998. Atmospheric iron supply and enhanced vertical carbon flux in the NE
691 subarctic Pacific: is there a connection? Global Biogeochemical Cycles 12 (3),
692 429-441.
- 693 Broecker, W.S., 1974. "NO", a conservative water-mass tracer. Earth and Planetary
694 Science Letters 23 (1), 100-107.
- 695 Carpenter, J.H., 1965. The Chesapeake Bay Institute technique for the Winkler dissolved
696 oxygen method. Limnology and Oceanography 10 (1), 141-143.
- 697 Castro, C.G., Chavez, F.P., Collins, C.A., 2001. Role of the California Undercurrent in
698 the export of denitrified waters from the eastern tropical North Pacific. Global
699 Biogeochemical Cycles 15 (4), 819-830.
- 700 Clarke, D.R., 1993. Non-parametric multivariate analyses of changes in community
701 structure. Austral Ecology 18, 117-143.
- 702 Combes, V., Di Lorenzo, E., 2007. Intrinsic and forced interannual variability of the Gulf
703 of Alaska mesoscale circulation Progress in Oceanography 75 (2), 266-286,
704 doi:10.1016/j.pocean.2007.08.011.
- 705 Cooney, R., 1976. Zooplankton and micronekton studies in the Bering-Chukchi/Beaufort
706 Seas. Principal investigators' reports for the environmental assessment of the
707 Alaskan continental shelf 2.
- 708 Coyle, K.O., Pinchuk, A.I., 2005. Seasonal cross-shelf distribution of major zooplankton
709 taxa on the northern Gulf of Alaska shelf relative to water mass properties,
710 species depth preferences and vertical migration behavior. Deep-Sea Research
711 Part II: Topical Studies in Oceanography 52 (1-2), 217-245.
- 712 Crawford, W.R., 2002. Physical characteristics of Haida Eddies. Journal of
713 Oceanography 58 (5), 703-713.
- 714 Crawford, W.R., Brickley, P.J., Peterson, T.D., Thomas, A.C., 2005. Impact of Haida
715 eddies on chlorophyll distribution in the eastern Gulf of Alaska. Deep Sea
716 Research Part II 52 (7-8), 975-989.

717 Crawford, W.R., Brickley, P.J., Thomas, A.C., 2007. Mesoscale eddies dominate surface
718 phytoplankton in northern Gulf of Alaska *Progress in Oceanography* 75 (2), 287-
719 303 doi:10.1016/j.pocean.2007.08.016.

720 Crawford, W.R., Cherniawsky, J.Y., Foreman, M.G.G., Gower, J.F.R., 2002. Formation
721 of the Haida-1998 oceanic eddy. *Journal of Geophysical Research - Oceans* 107
722 (C7), 3069, doi:10.1029/2001JC000876.

723 Crawford, W.R., Whitney, F.A., 1999. Mesoscale eddy swirl with data in Gulf of
724 Alaska. *EOS* 80, 365,370.

725 Di Lorenzo, E., Foreman, M.G.G., Crawford, W.R., 2005. Modelling the generation of
726 Haida Eddies. *Deep Sea Research Part II: Topical Studies in Oceanography* 52 (7-
727 8), 853-873.

728 Ducet, N., Le Traon, P.Y., Reverdin, G., 2000. Global high-resolution mapping of ocean
729 circulation from TOPEX/Poseidon and ERS-1 and-2. *Journal Of Geophysical
730 Research-Oceans* 105 (C8), 19477-19498.

731 Favorite, F., Dodimead, A.J., Nasu, K., 1976. Oceanography of the subarctic Pacific
732 region, 1960-71. *International North Pacific Fisheries Commission, Bulletin* 33,
733 187.

734 Fu, G., Baith, K.S., McClain, C.R., 1998. SeaDAS: The SeaWiFS Data Analysis System.
735 *Proceedings of The 4th Pacific Ocean Remote Sensing Conference, Qingdao,
736 China, 73-79.*

737 Gardner, G.A., Szabo, I., 1982. *British Columbia pelagic marine copepoda: An
738 identification manual and annotated bibliography.* E.V.S. Consultants Ltd.,
739 Marine Technology Center, Sidney, BC.

740 Gordon, H.R., Wang, M., 1994. Retrieval of water-leaving radiance and aerosol optical
741 thickness over the oceans with SeaWiFS: a preliminary algorithm. *Appl. Opt.* 33,
742 443-452.

743 Gower, J.F.R., 1989. Geosat altimeter observations of the distribution and movement of
744 sea-surface height anomalies in the north-east Pacific. *Oceans 89: the global
745 ocean.* Institute of Electrical and Electronics Engineers, Seattle, Washington, pp.
746 977-981.

747 Gower, J.F.R., Tabata, S., 1993. Measurement of eddy motion in the north-east Pacific
748 using the Geosat altimeter. In: Jones, Sugimori, Stewart (Eds.), *The 1st Pacific
749 Ocean Remote Sensing Conference.* PORSEC, Okinawa, Japan, pp. 375-382.

750 Henson, S.A., Thomas, A.C., 2008. A census of oceanic anticyclonic eddies in the Gulf
751 of Alaska. *Deep Sea Research Part I* 55 (2), 163-176
752 doi:10.1016/j.dsr.2007.11.005.

753 Incze, L.S., Siefert, D., Napp, J.M., 1997. Mesozooplankton of Shelikof Strait, Alaska:
754 abundance and community composition. *Continental Shelf Research* 17 (3), 287-
755 305.

756 Johnson, W.K., Miller, L.A., Sutherland, N.E., Wong, C.S., 2005. Iron transport by
757 mesoscale Haida eddies in the Gulf of Alaska. *Deep Sea Research Part II: Topical
758 Studies in Oceanography* 52 (7-8), 933-953.

759 Ladd, C., 2007. Interannual variability of the Gulf of Alaska eddy field. *Geophysical
760 Research Letters* 34 (11), L11605, doi:10.1029/2007GL029478.

761 Ladd, C., Kachel, N.B., Mordy, C.W., Stabeno, P.J., 2005a. Observations from a Yakutat
762 eddy in the northern Gulf of Alaska. *Journal Of Geophysical Research-Oceans*
763 110 (C3), C03003, doi: 10.1029/2004JC002710.

764 Ladd, C., Mordy, C.W., Kachel, N.B., Stabeno, P.J., 2007. Northern Gulf of Alaska
765 eddies and associated anomalies. *Deep Sea Research Part I* 54 (4), 487-509,
766 doi:10.1016/j.dsr.2007.01.006.

767 Ladd, C., Stabeno, P., Cokelet, E.D., 2005b. A note on cross-shelf exchange in the
768 northern Gulf of Alaska. *Deep Sea Research Part II* 52 (5-6), 667-679.

769 Le Traon, P.Y., Dibarboure, G., 1999. Mesoscale mapping capabilities of multi-satellite
770 altimeter missions. *Journal of Atmospheric and Oceanic Technology* 16, 1208-
771 1223.

772 Le Traon, P.Y., Dibarboure, G., 2004. An illustration of the contribution of the
773 TOPEX/Poseidon-Jason-1 tandem mission to mesoscale variability studies.
774 *Marine Geodesy* 27, 3-13.

775 Le Traon, P.Y., Nadal, F., Ducet, N., 1998. An improved mapping method of multi-
776 satellite altimeter data. *Journal of Atmospheric and Oceanic Technology* 15, 522-
777 534.

778 Lorenzen, C.J., 1966. A method for the continuous measurement of *in vivo* chlorophyll
779 concentration. *Deep Sea Research* 13 (2), 223-227.

780 Mackas, D.L., Galbraith, M.D., 2002. Zooplankton distribution and dynamics in a North
781 Pacific eddy of coastal origin: 1. Transport and loss of continental margin species.
782 *Journal of Oceanography* 58 (5), 725-738.

783 Mackas, D.L., Tsurumi, M., Galbraith, M.D., Yelland, D.R., 2005. Zooplankton
784 distribution and dynamics in a North Pacific Eddy of coastal origin: II.
785 Mechanisms of eddy colonization by and retention of offshore species. *Deep Sea*
786 *Research Part II* 52 (7-8), 1011-1035.

787 Martin, J., Gordon, R., Fitzwater, S., Broenkow, W., 1989. VERTEX: Phytoplankton/iron
788 studies in the Gulf of Alaska. *Deep Sea Research* 36 (5A), 649-680.

789 Martin, J.H., Gordon, R.M., 1988. Northeast Pacific iron distributions in relation to
790 phytoplankton productivity. *Deep-Sea Research* 35 (2 A), 177-196.

791 Melsom, A., Meyers, S.D., Hurlburt, H.E., Metzger, J.E., O'Brien, J.J., 1999. ENSO
792 effects on Gulf of Alaska eddies. *Earth Interactions* 3 (1), 1-30.

793 Murray, C.P., Morey, S.L., O'Brien, J.J., 2001. Interannual variability of upper ocean
794 vorticity balances in the Gulf of Alaska. *Journal of Geophysical Research -*
795 *Oceans* 106 (C3), 4479-4491.

796 Musgrave, D.L., Weingartner, T.J., Royer, T.C., 1992. Circulation and hydrography in
797 the northwestern Gulf of Alaska. *Deep Sea Research* 39 (9A), 1499-1519.

798 O'Reilly, J.E., Maritorena, S., Siegel, D.A., O'Brien, M.C., Toole, D., Chavez, F.P.,
799 Strutton, P., G.F. Cota, S.B. Hooker, C.R. McClain, K.L. Carder, F. Muller-
800 Karger, L. Harding, A. Magnuson, D. Phinney, G.F. Moore, J. Aiken, K.R.
801 Arrigo, R. Letelier, Culver, M., 2000. Ocean Chlorophyll a Algorithms for
802 SeaWiFS, OC2, and OC4: Version 4. In: O'Reilly, J.E., 24 Coauthors (Eds.),
803 SeaWiFS Postlaunch Calibration and Validation Analyses, Part 3, NASA Tech.
804 Memo. 2000-206892. NASA Goddard Space Flight Center, Greenbelt, MD, pp. 9-
805 19.

806 Okkonen, S.R., Jacobs, G.A., Metzger, E.J., Hurlburt, H.E., Shriver, J.F., 2001.
807 Mesoscale variability in the boundary currents of the Alaska Gyre. *Continental*
808 *Shelf Research* 21 (11-12), 1219-1236.

809 Okkonen, S.R., Weingartner, T.J., Danielson, S.L., Musgrave, D.L., Schmidt, G.M.,
810 2003. Satellite and hydrographic observations of eddy-induced shelf-slope
811 exchange in the northwestern Gulf of Alaska. *Journal of Geophysical Research*
812 108 (C2), 3033, doi:10.1029/2002JC001342.

813 Onishi, H., Ohtsuka, S., Anma, G., 2000. Anticyclonic, baroclinic eddies along 145°W in
814 the Gulf of Alaska in 1994-1999. *Bulletin of the Faculty of Fisheries, Hokkaido*
815 *University* 51 (1), 31-43.

816 Peterson, T.D., Whitney, F.A., Harrison, P.J., 2005. Macronutrient dynamics in an
817 anticyclonic mesoscale eddy in the Gulf of Alaska. *Deep Sea Research Part II:*
818 *Topical Studies in Oceanography* 52 (7-8), 909-932.

819 Roden, G.I., 1964. Shallow temperature inversions in the Pacific Ocean. *Journal of*
820 *Geophysical Research* 69, 2899-2914.

821 Shettle, E.P., Fenn, R.W., 1979. Models for the Aerosols for the Lower Atmosphere and
822 the Effects of Humidity Variations on Their Optical Properties. AFGL-TR-79-
823 0214 Environmental Research Papers No. 676.

824 SSALTO/DUACS, 2006. SSALTO/DUACS User Handbook: (M)SLA and (M)ADT
825 Near-Real Time and Delayed Time Products, Ramonville St-Agne, France.

826 Stabeno, P., Bond, N.A., Hermann, A.J., Kachel, N.B., Mordy, C.W., Overland, J.E.,
827 2004. Meteorology and oceanography of the northern Gulf of Alaska. *Continental*
828 *Shelf Research* 24 (7-8), 859-897.

829 Swaters, G.E., Mysak, L.A., 1985. Topographically-induced baroclinic eddies near a
830 coastline, with application to the Northeast Pacific. *Journal of Physical*
831 *Oceanography* 15 (11), 1470-1485.

832 Tabata, S., 1982. The anticyclonic, baroclinic eddy off Sitka, Alaska, in the northeast
833 Pacific Ocean. *Journal of Physical Oceanography* 12 (11), 1260-1282.

834 Uda, M., 1963. Oceanography of the subarctic Pacific Ocean. *J. Fish. Res. Board Can.*
835 20, 119-179.

836 Ueno, H., Oka, E., Suga, T., Onishi, H., Roemmich, D., 2007. Formation and variation of
837 temperature inversions in the eastern subarctic North Pacific. *Geophysical*
838 *Research Letters* 34, L05603, doi:10.1029/2006GL028715.

839 Ueno, H., Yasuda, I., 2000. Distribution and formation of the mesothermal structure
840 (temperature inversions) in the North Pacific subarctic region. *Journal of*
841 *Geophysical Research - Oceans* 105 (C7), 16,885–816,898.

842 Ueno, H., Yasuda, I., 2001. Warm and saline water transport to the North Pacific
843 subarctic region: World Ocean Circulation Experiment and Subarctic Gyre
844 Experiment data analysis. *Journal of Geophysical Research - Oceans* 106 (C10),
845 22,131–122,142.

846 Ueno, H., Yasuda, I., 2003. Intermediate water circulation in the North Pacific subarctic
847 and northern subtropical regions. *Journal of Geophysical Research - Oceans* 108
848 (C11), 3348, doi:10.1029/2002JC001372.

849 Ueno, H., Yasuda, I., 2005. Temperature inversions in the subarctic North Pacific.
850 *Journal of Physical Oceanography* 35 (12), 2444-2456.

851 Whitney, F., Freeland, H.J., Robert, M., 2007. Persistently declining oxygen levels in the
852 interior waters of the eastern subarctic Pacific. *Progress in Oceanography* 75, 179-
853 199.

854 Whitney, F., Robert, M., 2002. Structure of Haida eddies and their transport of nutrient
855 from coastal margins into the NE Pacific Ocean. *Journal of Oceanography* 58 (5),
856 715-723.

857 Whitney, F.A., Crawford, D.W., Yoshimura, T., 2005. The uptake and export of silicon
858 and nitrogen in HNLC waters of the NE Pacific Ocean. *Deep Sea Research Part*
859 *II: Topical Studies in Oceanography* 52 (7-8), 1055-1067.

860 Whitney, F.A., Welch, D.W., 2002. Impact of the 1997–1998 El Niño and 1999 La Niña
861 on nutrient supply in the Gulf of Alaska. *Progress in Oceanography* 54 (1-4), 405-
862 421.

863
864
865

866 **Figure Captions.**

867 Figure 1. Schematic of Alaskan Gyre circulation. Black dots show locations of CTD
868 stations. Dashed line shows approximate boundary of dilute domain. Shelf region (depth
869 < 200m) shown with gray shading. Inset shows location of stations and ship track in the
870 eastern GOA. CTD casts were taken at each station. Select cast numbers are noted.
871 Black filled circles show locations of deep Fe casts. Grey filled circles show locations of
872 shallow Fe casts.

873 Figure 2. Altimeter SSHA data in cm (color) and drifter trajectories (5-day tails: black
874 lines). Drifters travel clockwise around these anticyclonic eddies. Blue line in final panel
875 shows cruise track (26 April – 8 May 2005). Note that timing of cruise is not exactly
876 coincident with altimetry data shown. In particular, by 18 May, the Haida eddy had
877 moved north from where it was sampled.

878 Figure 3. Temperature (top) and salinity (bottom) observed in the Haida transect (left)
879 and the Sitka/Yakutat transect (right). Density contours overlaid in black. Red line
880 denotes mixed layer depth. Arrows at the top of the plots show location of stations.
881 Numbers denote cast number. Horizontal axis shows distance (km) from the center of the
882 Haida eddy (left) or the Sitka eddy (right).

883 Figure 4. MODIS chlorophyll data (8-day composite centered on 6 May 2005). Ship
884 track is overlaid (black line). Locations of select casts are denoted by circles and cast
885 numbers.

886 Figure 5. Background colors (blue/green scale) represent chlorophyll concentrations in
887 the top 50m. Colored dots represent nitrate. Note that the nitrate color scale for the top
888 50m is different from the scale for the deeper water. Density contours overlaid in black.

889 Figure 6. Silicic acid vs. nitrate (top) and phosphate vs. nitrate (bottom) for all of the
890 casts (depth = 0 – 200m) in the Haida transect (red), and the Sitka/Yakutat transect
891 (blue), except casts 47 – 54 (center of Yakutat eddy; green).

892 Figure 7. Nitrate (μM) vs. salinity for Haida transect (red symbols) and Sitka/Yakutat
893 transect (blue symbols) (depth = 0 – 1000m). Lines represent the cast nearest the center
894 of each eddy (Haida cast 10 = red; Sitka cast 39 = blue; and Yakutat cast 52 = green) and
895 the Reference cast 1 (black).

896 Figure 8. Data from the center stations of the three eddies in April/May (cast numbers
897 noted in legend) and from the Haida eddy, OSP, and a station in Queen Charlotte Sound
898 in June 2005. (a) Nitrate, (b) dissolved oxygen, and (c) NO.

899 Figure 9. Profiles of temperature ($^{\circ}\text{C}$; black), salinity (blue), and total iron content (nM;
900 red) for the casts nearest the center of the three eddies. Iron content at the reference cast
901 (cast 1) is also shown in Haida plots and noted with arrow. Bottom plots are same data
902 with density (σ_{θ}) as the vertical axis. Gray shading illustrates the depth (density) range of
903 the eddy core waters (Table 3). Note that the iron measurements were taken separately
904 from the temperature and salinity casts so the data in each plot were not obtained
905 concurrently. However data in each plot are from the same location and obtained within
906 ~1 day of each other.

907 Table 1. Drifters deployed in the three eddies.

Drifter Number	Eddy deployed in	Date Deployed	Ship deployed from
53319	Haida	13 March 2005	<i>CCGS W.E. Ricker</i>
53309	Haida	23 April 2005	<i>CCGS W.E. Ricker</i>
53312	Haida	23 April 2005	<i>CCGS W.E. Ricker</i>
53310	Haida	30 April 2005	<i>R/V Thomas G. Thompson</i>
53308	Sitka	3 May 2005	<i>R/V Thomas G. Thompson</i>
53321	Sitka	3 May 2005	<i>R/V Thomas G. Thompson</i>
53304	Yakutat	6 May 2005	<i>R/V Thomas G. Thompson</i>
53306	Yakutat	6 May 2005	<i>R/V Thomas G. Thompson</i>

908

909 Table 2. Eddy formation dates and age when sampled.

	Eddy formation date from altimetry	Dates Sampled	Age of eddy when sampled
Haida	10 January 2005	28 April – 1 May 2005	3.5 months
Sitka	22 December 2004	2 May – 5 May 2005	4.5 months
Yakutat	23 March 2005	6 – 7 May 2005	1.5 months

910

911 Table 3. Eddy core water properties.

	Surface Mixed Layer			Subsurface Core		
	Haida	Sitka	Yakutat	Haida	Sitka	Yakutat
Depth range (m)	0 – 56	0 – 10	0 – 11	100 – 550	110 – 550	110 – 335
Density Range (σ_θ)	25.0 – 25.1	24.9 – 25.0	24.7 – 24.9	25.6 – 26.8	25.4 – 26.8	25.3 – 26.7
Temperature ($^\circ\text{C}$)	8.26	8.39	8.74	6.63	6.11	6.44
Salinity	32.14	32.03	31.95	33.79	33.55	33.20
Nitrate (μM)	10.40	6.90	13.95	33.68	31.62	27.30
Silicic Acid (μM)	16.89	11.46	27.87	54.13	53.00	42.48
Phosphate (μM)	1.14	0.96	1.36	2.54	2.38	2.13
Total Fe (nM)	0.9	0.5	1.8	14.0	11.5	29.9
Labile Fe (nM)	0.35	0.20	0.77	3.72	2.67	4.56
Chlorophyll ($\mu\text{g l}^{-1}$) 1)	0.29	1.94	0.47	No data	No data	No data

912

913 Table 4: SIMPER analysis

914 Average zooplankton abundance (estimated number m⁻³) in the Sitka and Haida eddies.

915

916 Average Dissimilarity = 17.36

Species Group	Haida Eddy	Sitka Eddy	% Contribution to Dissimilarity
Euphausiid calyptopes, nauplii and furcilia	8.43	79.82	10.88
<i>Acartia</i> spp. (adult)	4.17	23.34	7.62
Thecosomata	212.15	165.62	7.24
Larvacea	12.00	24.63	6.91
<i>Oithona</i> spp. (CV + CVI)	248.91	412.13	6.68
<i>Neocalanus plumchrus / flemingeri</i> (CII – Adult)	15.03	54.07	5.99
Siphonophora	10.36	10.25	5.71
<i>Pseudocalanus</i> spp. (CI – Adult)	172.86	102.96	5.49
Cnidarian medusa	0.48	1.06	4.60
<i>Eucalanus bungii</i> (CI – Adult)	5.78	13.69	4.06
Teleost Larvae	0.18	0.30	3.82
Hyperideida	0.61	0.06	3.77
Cirripedia	0.73	1.47	3.56
<i>Calanus marshallae</i> (CII – Adult)	2.34	4.72	3.50
<i>Euphausia pacifica</i> (Adult + Juvenile)	0.16	0.02	3.19
<i>Calanus pacificus</i> (CIV – Adult)	0.47	0.06	3.14
Ostracoda	19.30	14.68	2.89
<i>Metridia pacifica / lucens</i> (CIV – Adult)	54.03	77.84	2.75

917

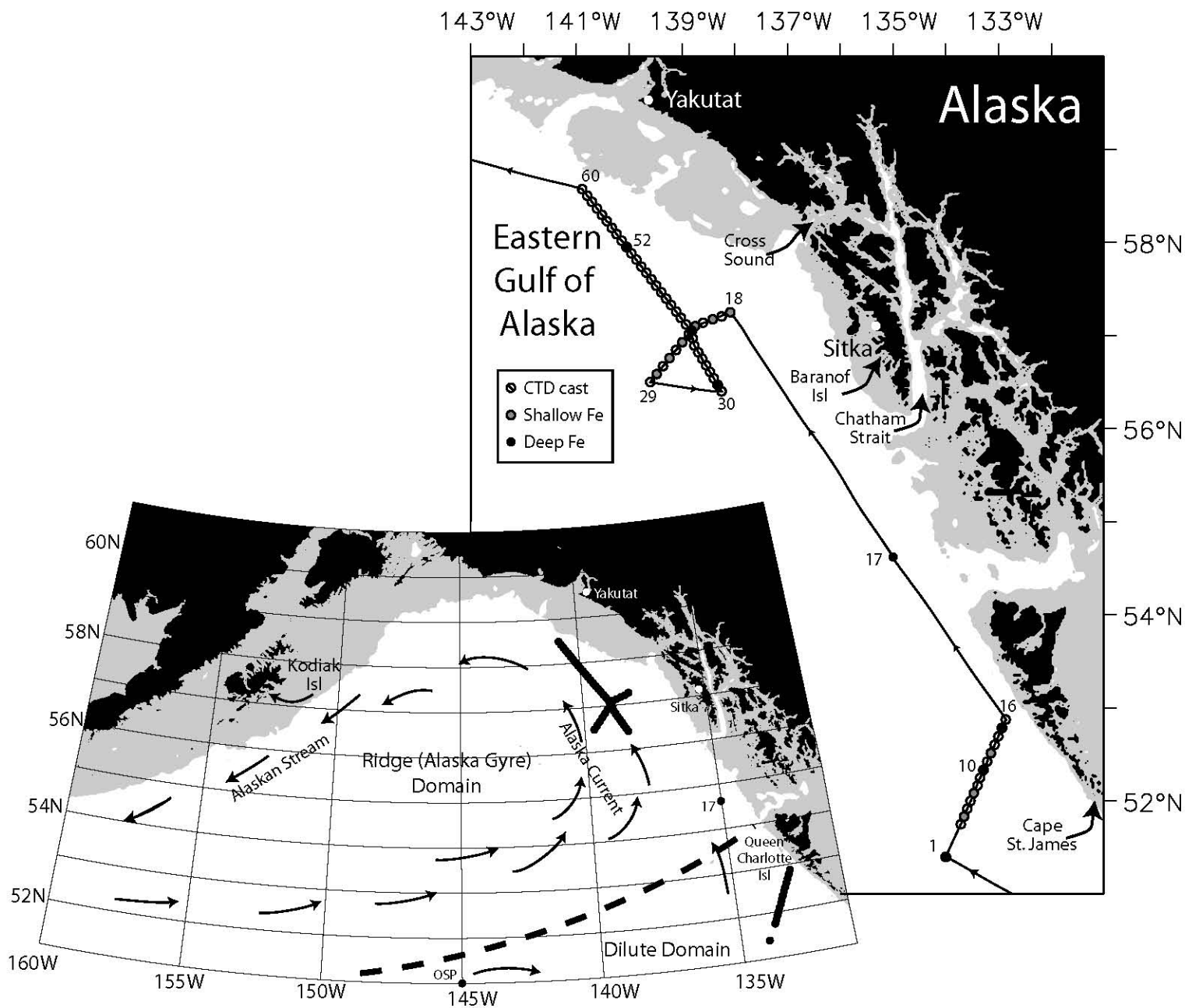


Figure 1. Schematic of Alaskan Gyre circulation. Black dots show locations of CTD stations. Dashed line shows approximate boundary of dilute domain. Shelf region (depth < 200m) shown with gray shading. Inset shows location of stations and ship track in the eastern GOA. CTD casts were taken at each station. Select cast numbers are noted. Black filled circles show locations of deep Fe casts. Grey filled circles show locations of shallow Fe casts.

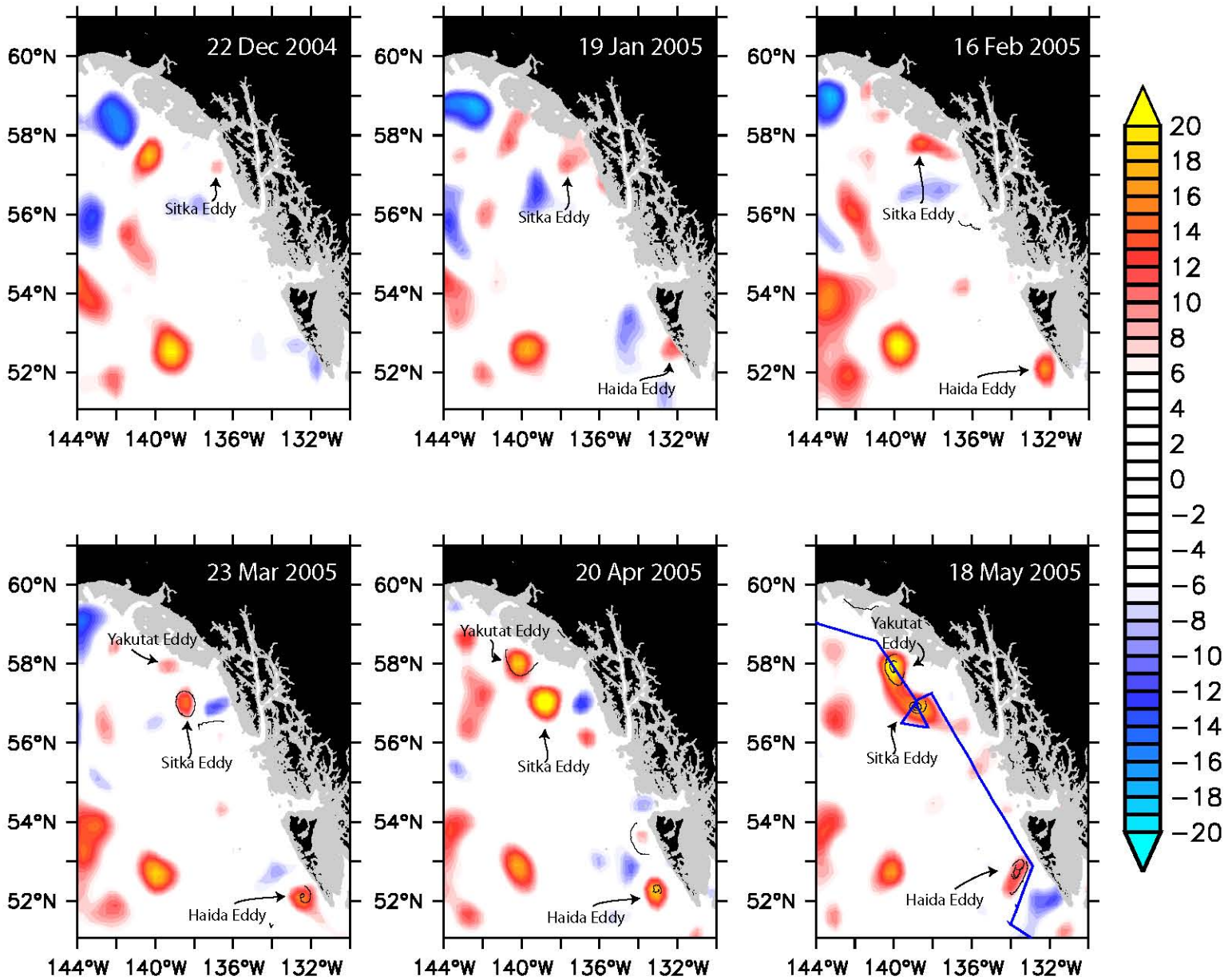


Figure 2. Altimeter SSHA data in cm (color) and drifter trajectories (5-day tails: black lines). Drifters travel clockwise around these anticyclonic eddies. Blue line in final panel shows cruise track (26 April - 8 May 2005). Note that timing of cruise is not exactly coincident with altimetry data shown. In particular, by 18 May, the Haida eddy had moved north from where it was sampled.

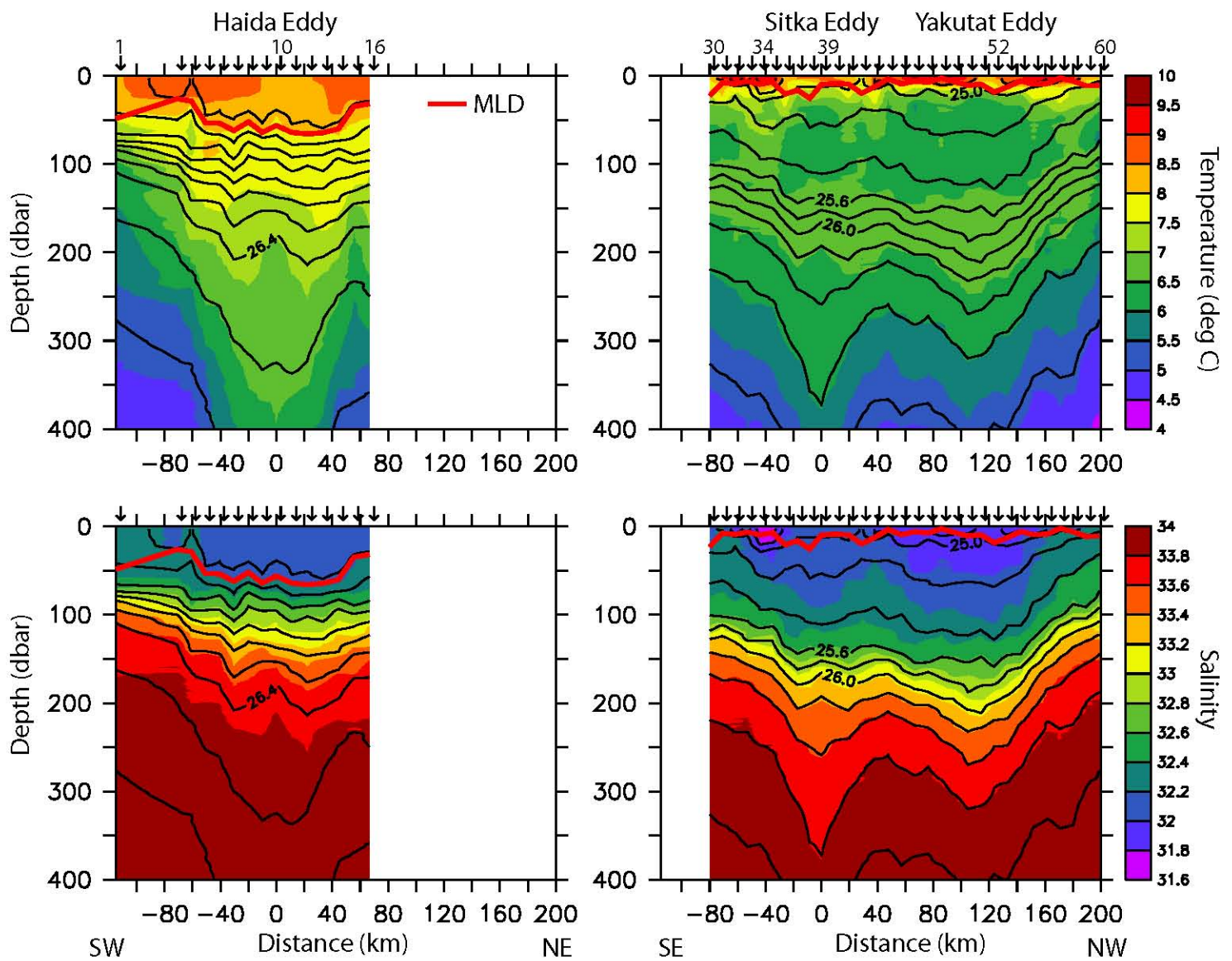
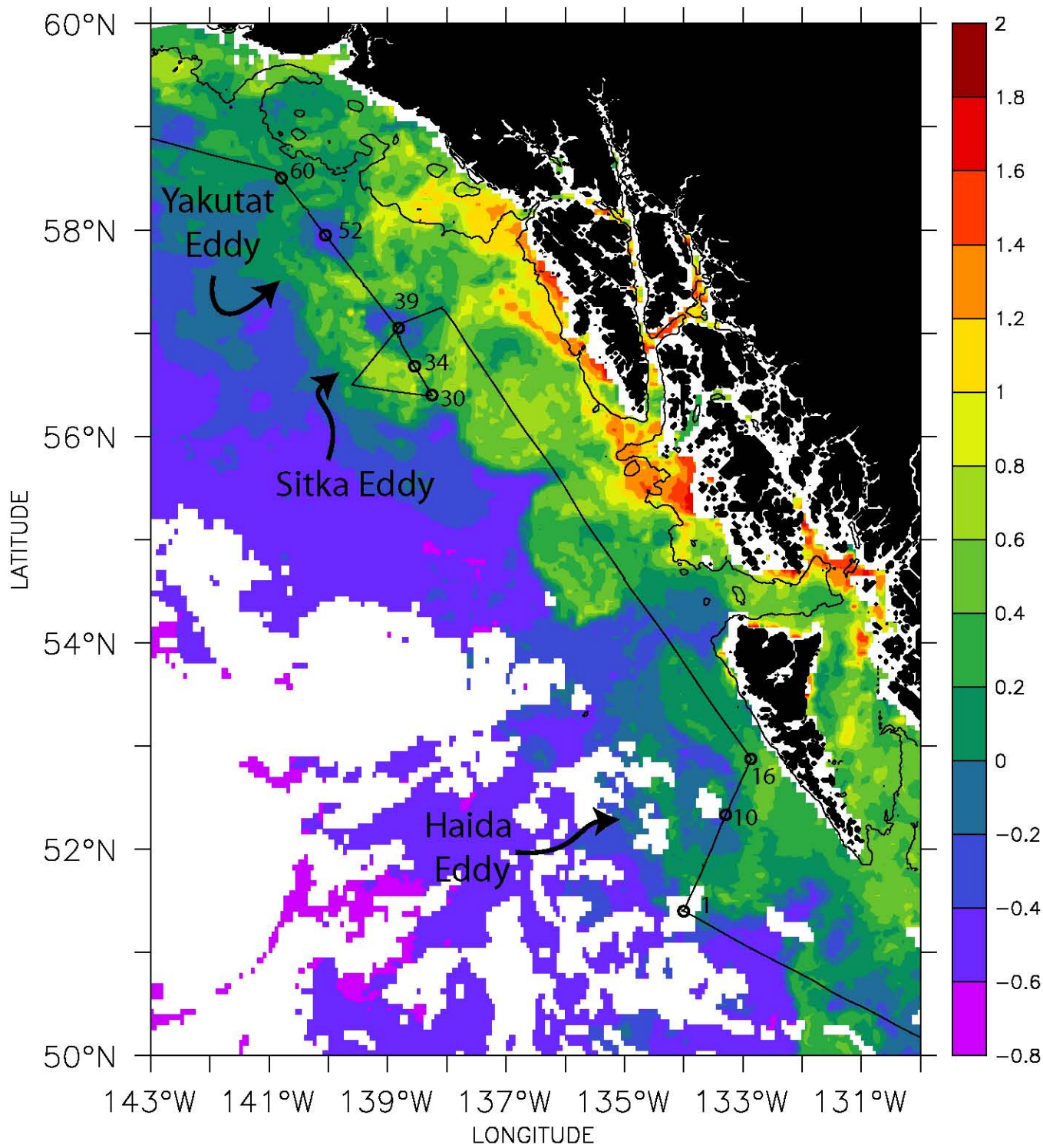


Figure 3. Temperature (top) and salinity (bottom) observed in the Haida transect (left) and the Sitka/Yakutat transect (right). Density contours overlaid in black. Red line denotes mixed layer depth. Arrows at the top of the plots show location of stations. Numbers denote cast number. Horizontal axis shows distance (km) from the center of the Haida eddy (left) or the Sitka eddy (right).



Chlorophyll a (log, mg m⁻³)

Figure 4. MODIS chlorophyll data (8-day composite centered on 6 May 2005). Ship track is overlaid (black line). Locations of select casts are denoted by circles and cast numbers.

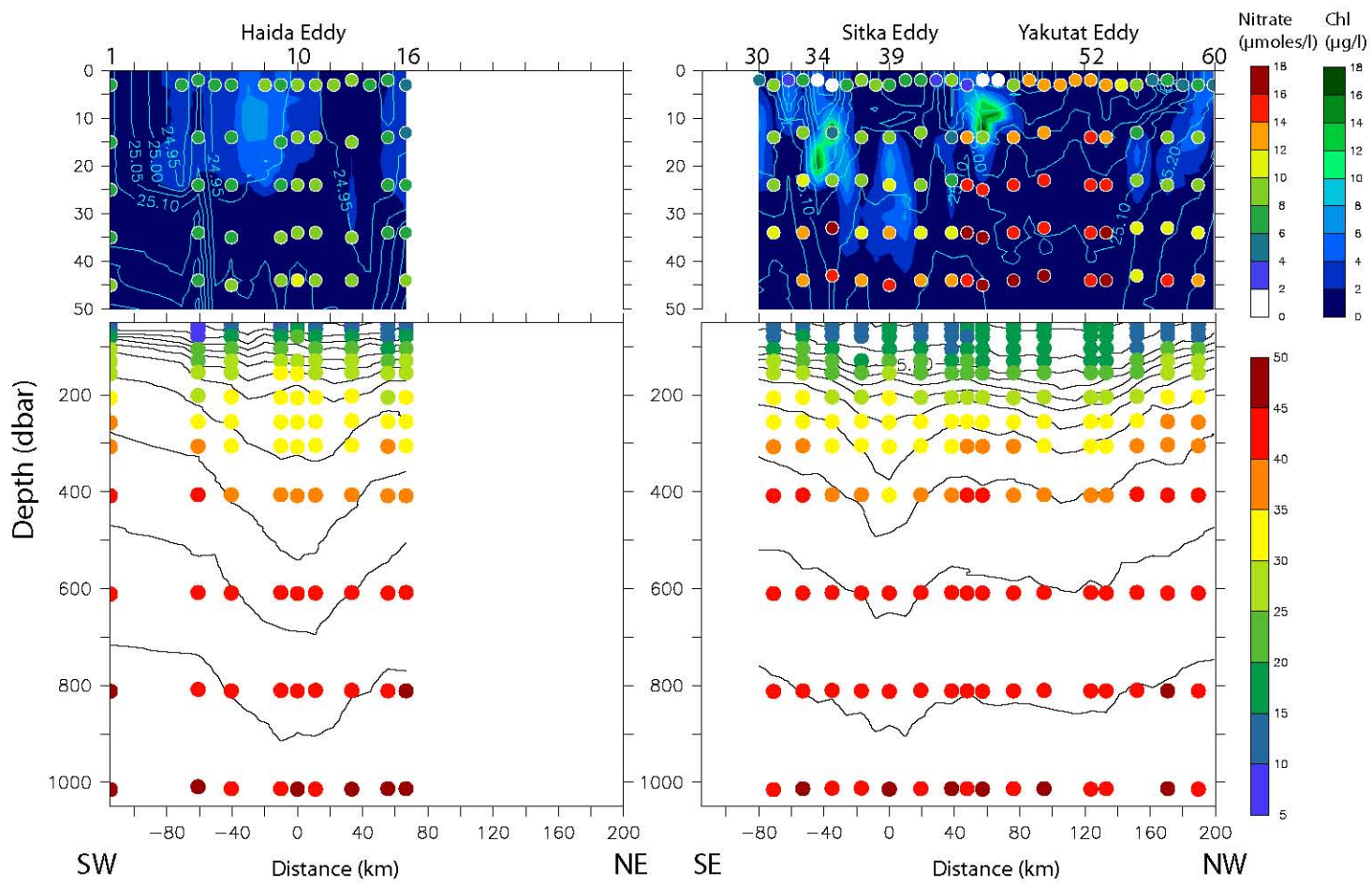


Figure 5. Background colors (blue/green scale) represent chlorophyll concentrations in the top 50m. Colored dots represent nitrate. Note that the nitrate color scale for the top 50m is different from the scale for the deeper water. Density contours overlaid in black.

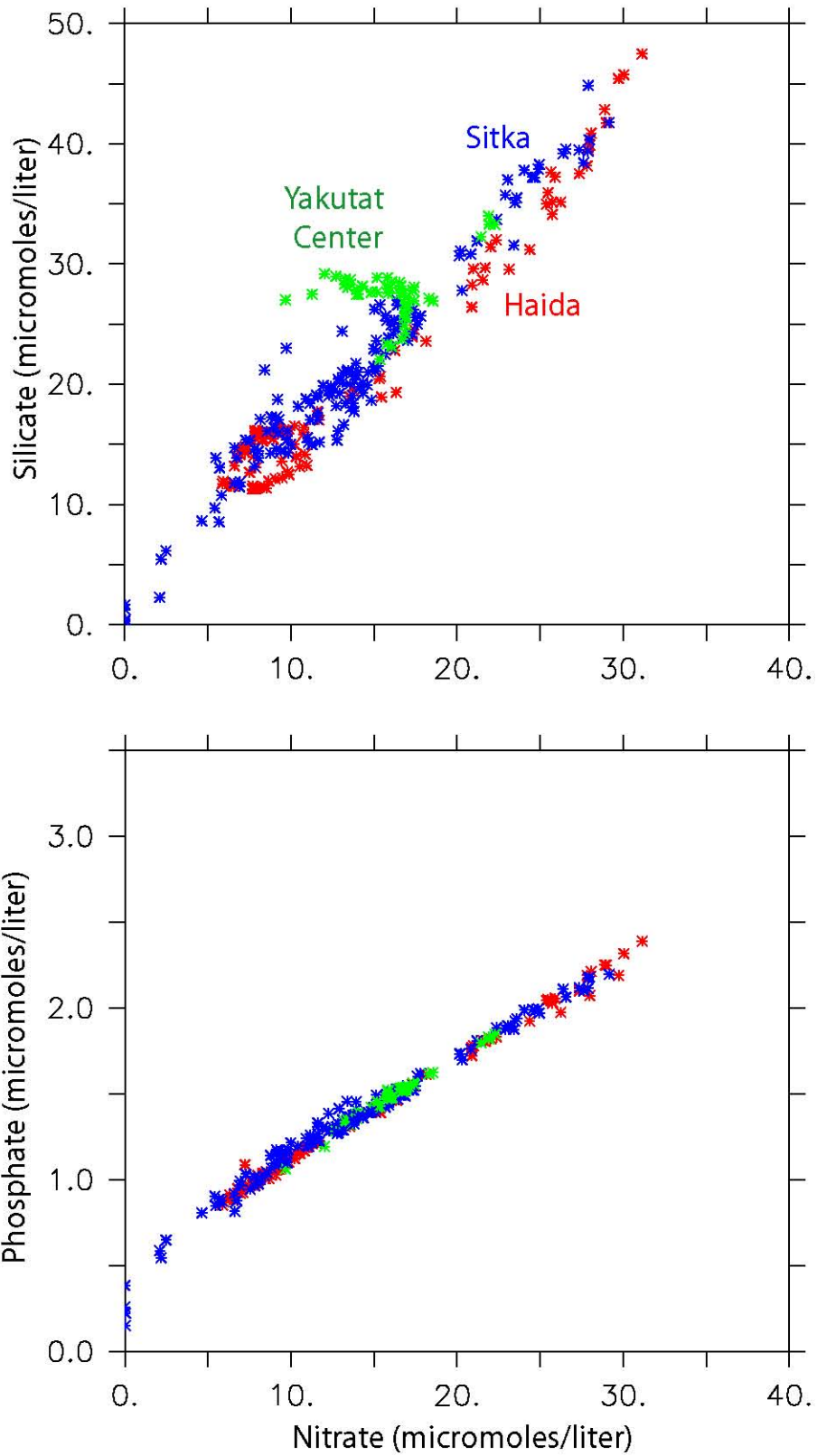


Figure 6. Silicic acid vs. nitrate (top) and phosphate vs. nitrate (bottom) for all of the casts (depth = 0 - 200m) in the Haida transect (red), and the Sitka/Yakutat transect (blue), except casts 47 - 54 (center of Yakutat eddy; green).

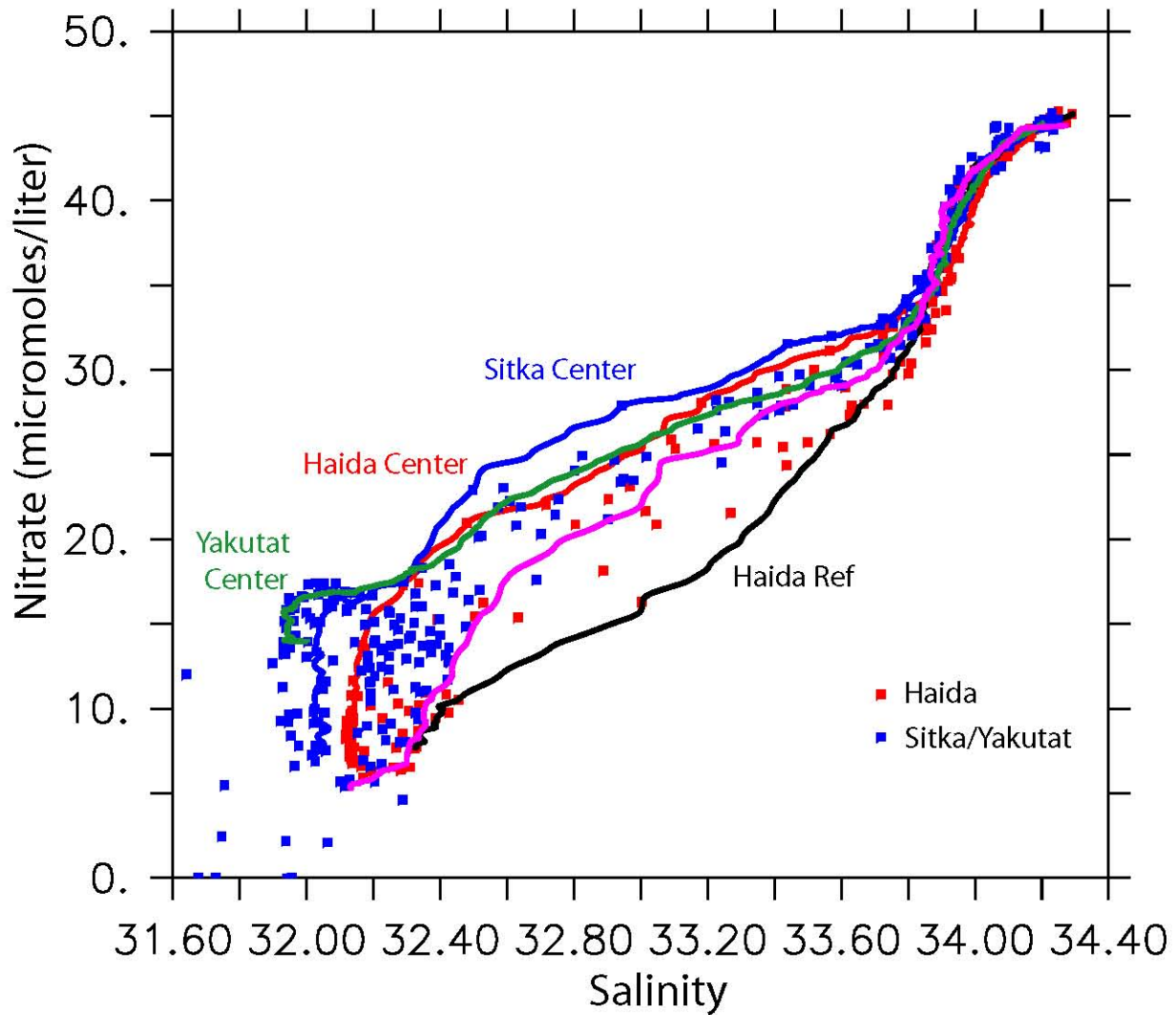


Figure 7. Nitrate (μM) vs. salinity for Haida transect (red symbols) and Sitka/Yakutat transect (blue symbols) (depth = 0 - 1000m). Lines represent the cast nearest the center of each eddy (Haida cast 10 = red; Sitka cast 39 = blue; and Yakutat cast 52 = green) and the Reference cast 1 (black).

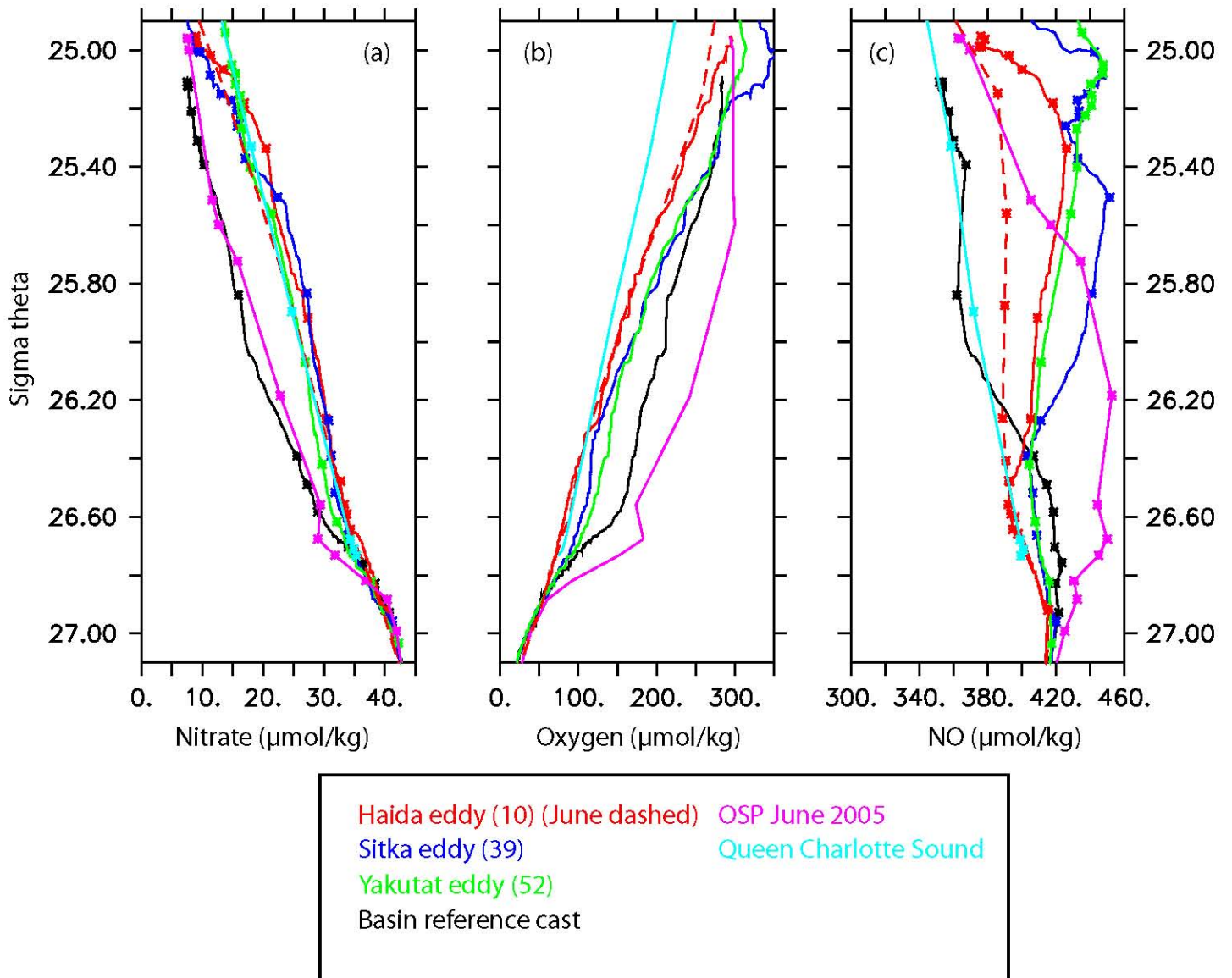


Figure 8. Data from the center stations of the three eddies in April/May (cast numbers noted in legend) and from the Haida eddy, OSP, and a station in Queen Charlotte Sound in June 2005. (a) Nitrate, (b) dissolved oxygen, and (c) NO.

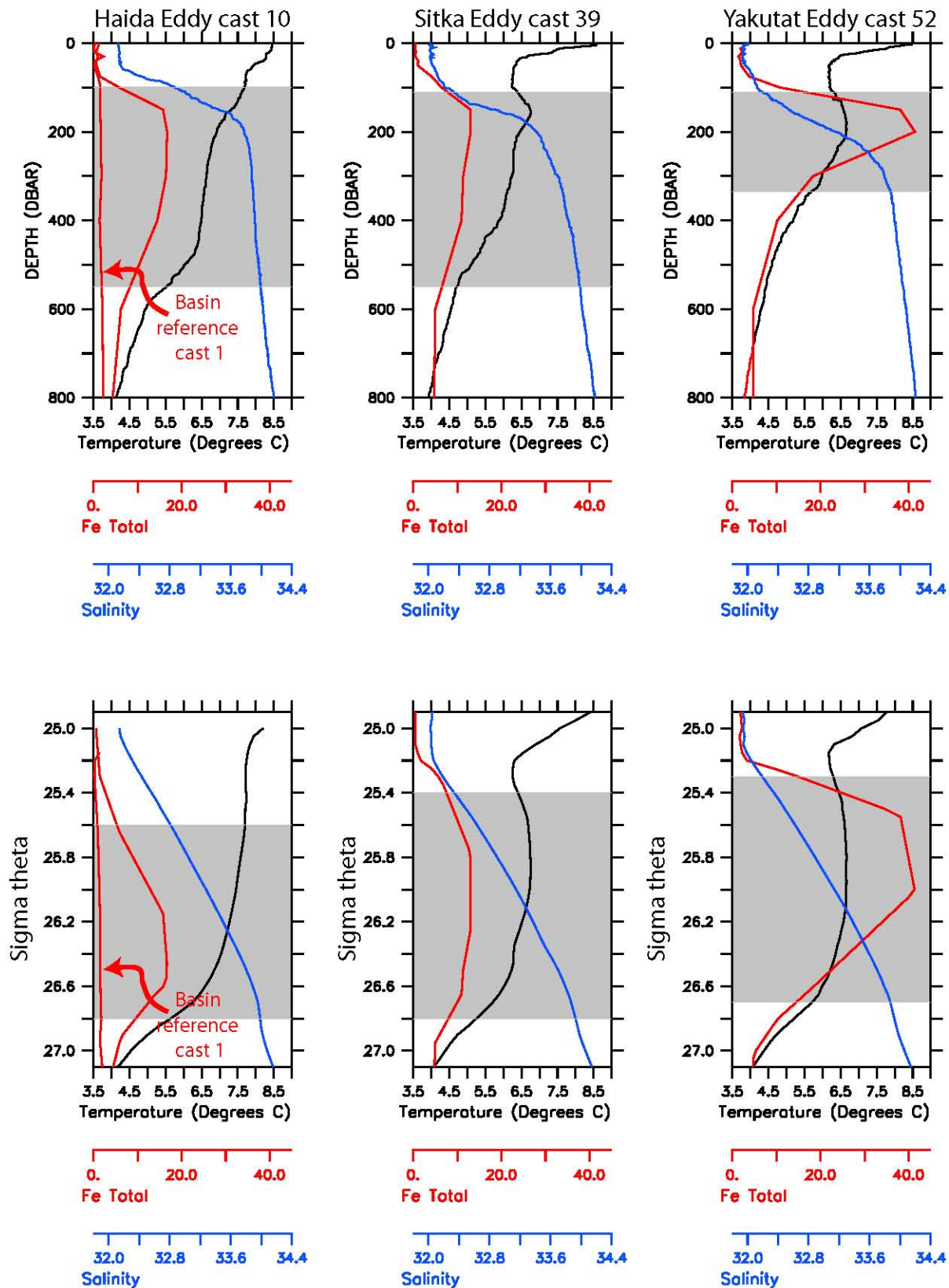


Figure 9. Profiles of temperature ($^{\circ}\text{C}$; black), salinity (blue), and total iron content (nM; red) for the casts nearest the center of the three eddies. Iron content at the reference cast (cast 1) is also shown in Haida plots and noted with arrow. Bottom plots are same data with density (σ_{θ}) as the vertical axis. Gray shading illustrates the depth (density) range of the eddy core waters (Table 3). Note that the iron measurements were taken separately from the temperature and salinity casts so the data in each plot were not obtained concurrently. However data in each plot are from the same location and obtained within ~ 1 day of each other.